Antihydrogen

Recombination processes in plasma

Binary recombination

$\alpha\,[\mathrm{cm^3 s^{-1}}]$

$H^+ + e \rightarrow H + h\nu$ — RR — radiative recombination

$O_2^+ + e \rightarrow O + O$ — DR — dissociative recombination

$$\frac{dn_e}{dt} = \frac{d[O_2^+]}{dt} = -\alpha[O_2^+]n_e = -\alpha n_e^2$$

$Fe^{7+} + e \rightarrow Fe^{6+}$ — DiR — dielectronic recombination

Ternary electron assisted recombination

$Ar^+ + e + e \rightarrow Ar + e$

$$\frac{dn_e}{dt} = \frac{d[Ar^+]}{dt} = -K_e[Ar^+]n_e^2 = -\alpha_{eff}[Ar^+]n_e$$

Collisional Radiative Recombination

CRR

$K_{CRR}\,[\mathrm{cm^6 s^{-1}}]$

$\alpha_{eff} = K_e n_e$

Ternary neutral assisted recombination

$Ar^+ + e + He \rightarrow Ar + He$

$$\frac{dn_e}{dt} = \frac{d[Ar^+]}{dt} = -K_M[Ar^+]n_e[He] = -\alpha_{eff}[Ar^+]n_e$$

$K_M\,[\mathrm{cm^6 s^{-1}}]$

$\alpha_{eff} = K_M[He]$

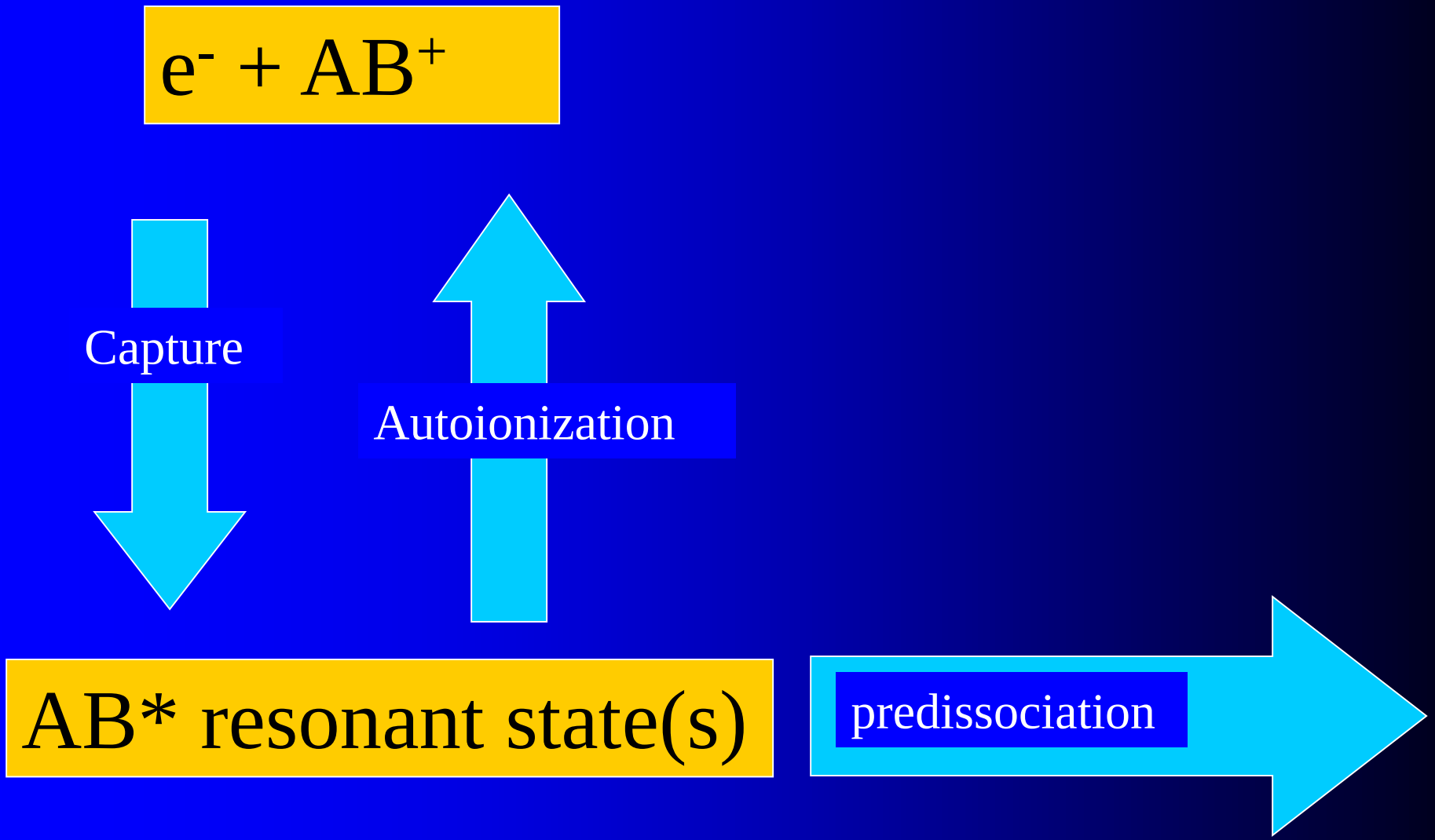

To get high recombination rate, we need

(a) efficient capture

(b) predissociation faster than auto-ionization

Electron-cold molecular ion reaction: Dissociative Recombination

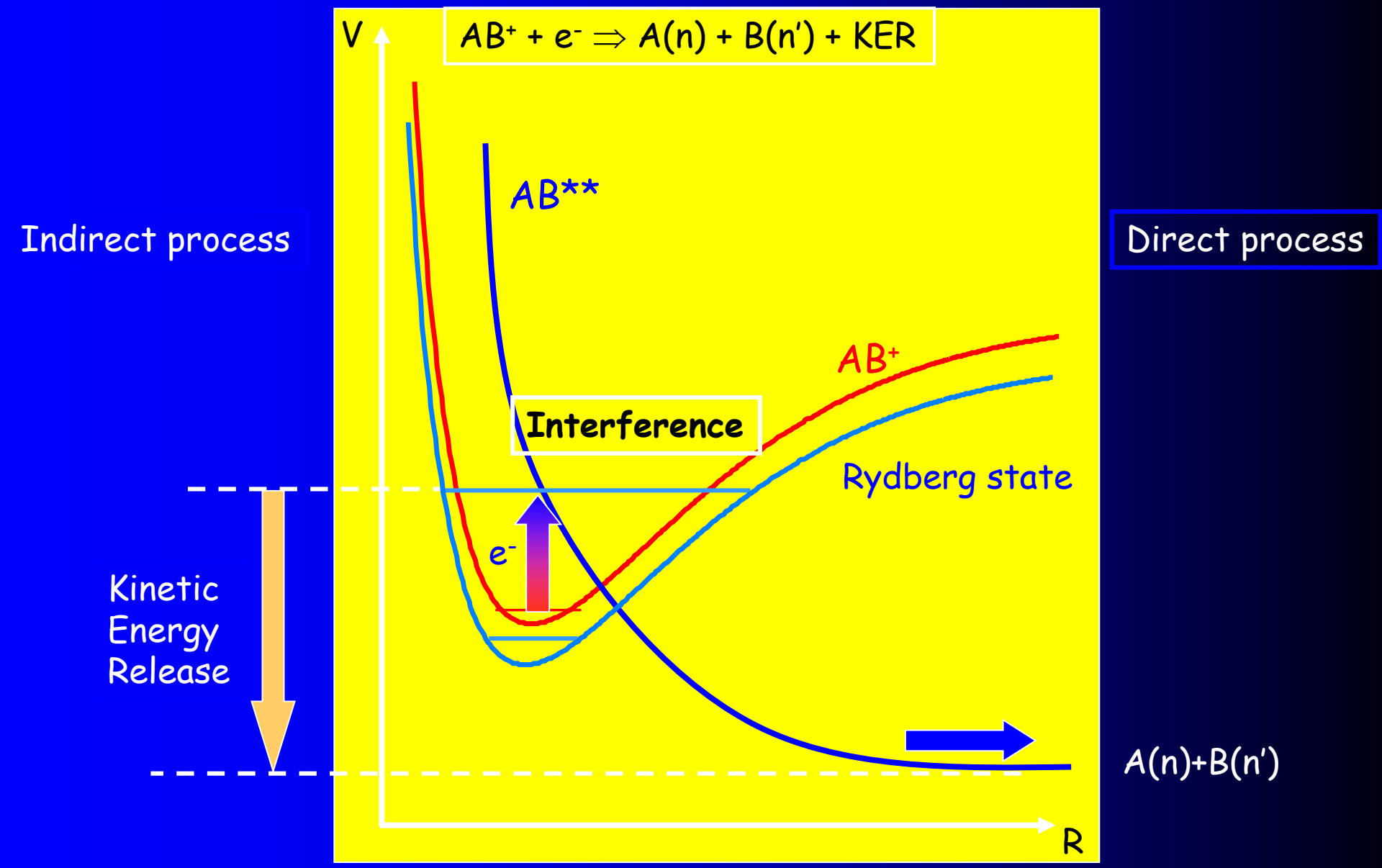

Recombination of H_3^+ : No ion-neutral crossing

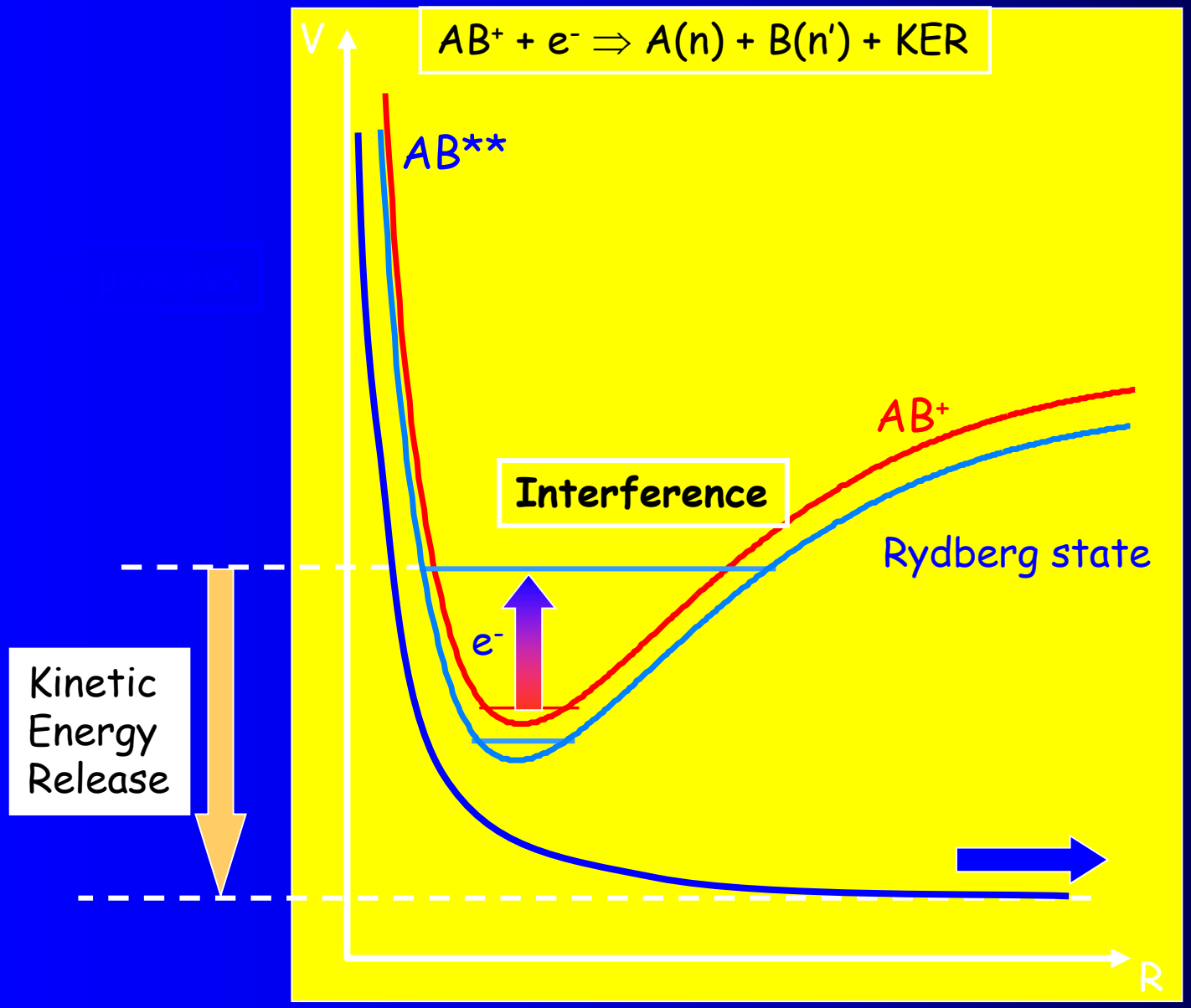

~~Direct process~~

The CRESU technique at Rennes

Carrier gas (He, Ar or N_2) + reactants

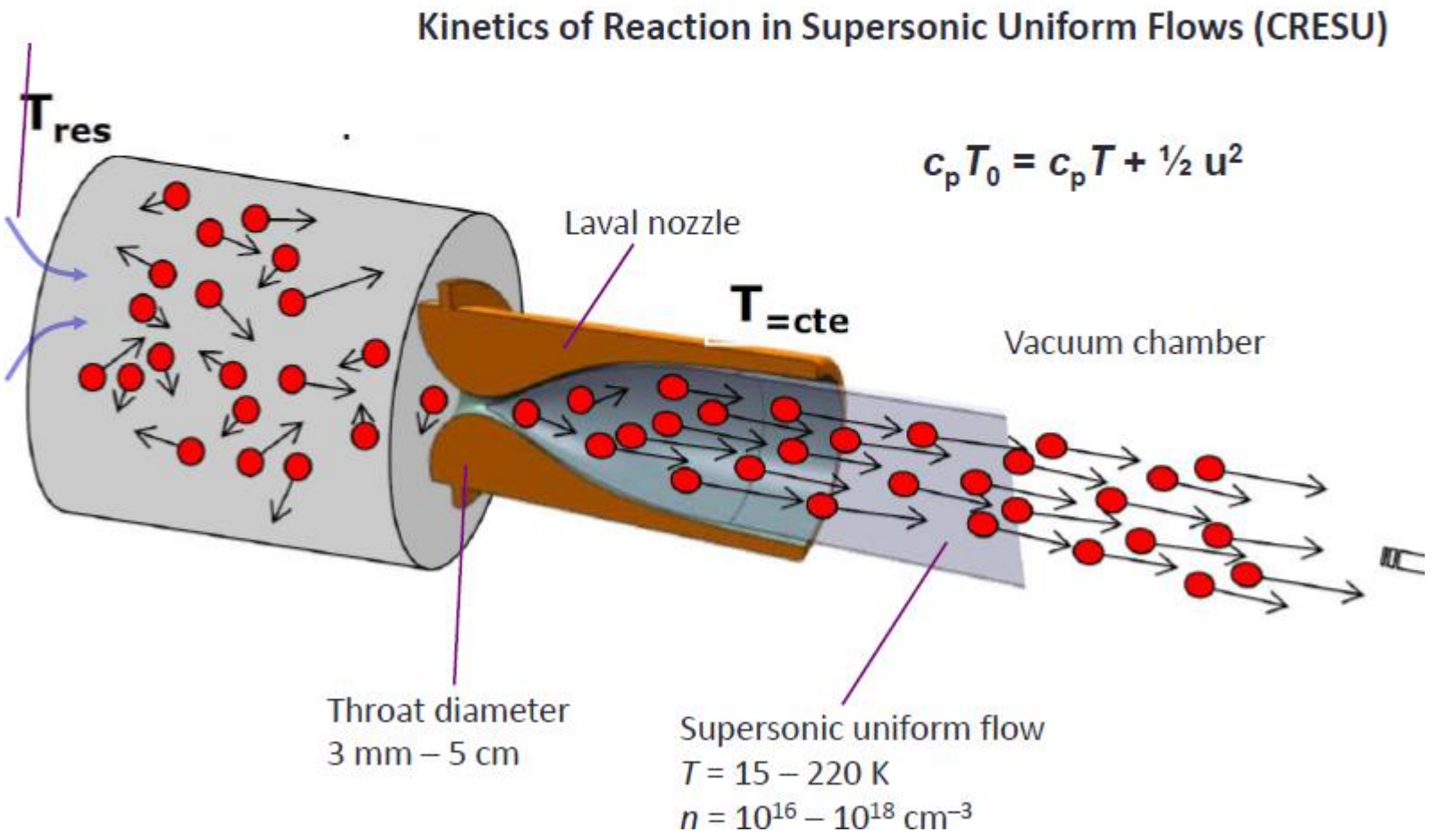

Motivation for Antihydrogen Experiments

Swansea University
Prifysgol Abertawe

| Antihydrogen | = | Hydrogen |

| ?

Gravity

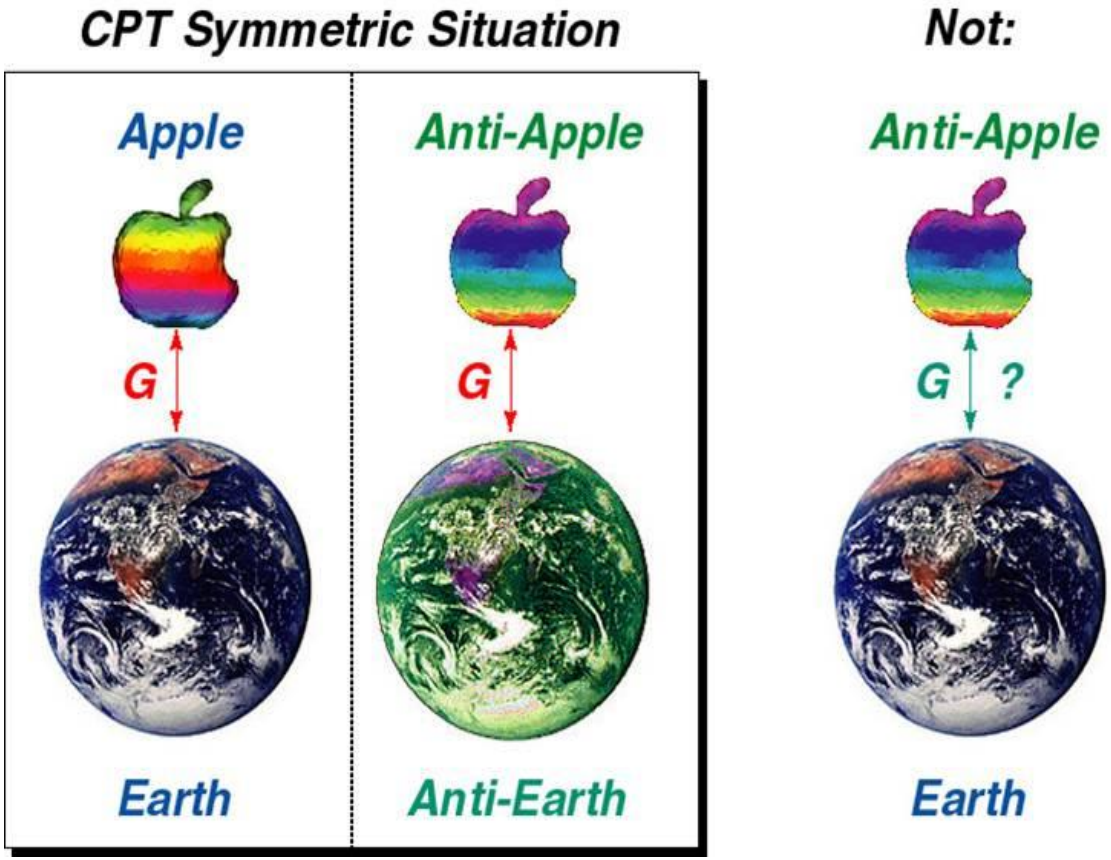

Gabrielse

Huge Energy Release!

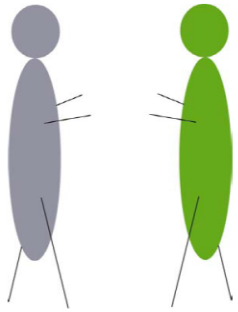

100 kg
Anti-Gabrielse

100 kg
Gabrielse

energy released

mass that disappears

200 kg

$E = mc^2$

Einstein's famous formula

5,000,000,000,000 kilowatt-hours
Yearly output of 500 nuclear power plants
Energy from 4200 Megatons of TNT

$$\text{Efficiency} = \frac{\text{Energy Released}}{\text{Mass of Fuel Used}}$$

Annihilation	100 %
Nuclear fission	0.1 %
Nuclear fusion	0.1 % (or a bit higher)
Chemical fuel	0.000 000 3 %

Annihilation

- 1000 times more bang for the gram compared to nuclear fuel

Energy Source of the Future?	No, certainly not
Antimatter Weapons?	No, certainly not
Antimatter Rockets?	Doubtful, … maybe in distant future

Production Methods

I. ANTIPROTON + POSITRON (exp.demonstration: ATHENA and ATRAP)

(A)

Spontaneous Radiative Recombination (SRR)

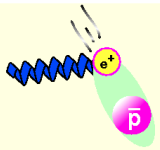

$\bar{p} + e^+ \rightarrow \bar{H} + h\nu$

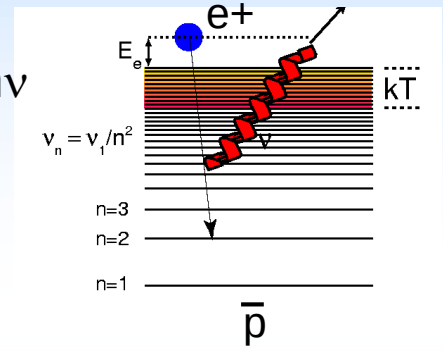

(B)

Three-Body Recombination (TBR)

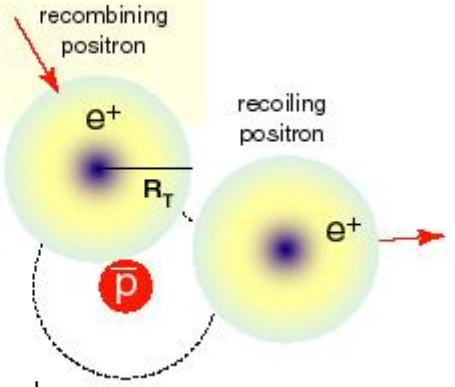

$\bar{p} + e^+ + e^+ \rightarrow \bar{H} + e^+$

EXPERIMENTAL RESULTS:

- TBR seems to be the dominant process (highly exicited antihydrogen)
- Warm antihydrogen atoms (production when $v_{antiproton} \sim v_{positron}$)

II. ANTIPROTON + RYDBERG POSITRONIUM (exp.demonstration: ATRAP)

$\bar{p} + Ps^* \rightarrow \bar{H} + e^-$

PROMISING TECHNIQUE:

- Control of the antihydrogen quantum state
- Cold antihydrogen atoms ($v_{antihydrogen} \sim v_{antiproton}$)

→ Production Method in AEGIS

Antimatter history in a slide

- 1928: relativistic equation of the ½ spin electron (Dirac)
- 1929: electron sea and hole theory (Dirac)
- 1931: prediction of antimatter (Dirac, Oppenheimer, Weyl)
- 1932: discovery of positron in cosmic rays (Anderson)
- 1933: discovery of e-/e+ creation and annihilation (Blackett, Occhialini)
- 1937: symmetric theory of electrons and positrons
- 1955: antiproton discovery (Segre', Chamberlain, Wiegand)
- 1956: antineutron discovery (Cork, Lambertson, Piccioni, Wenzel)
- 1995: creation of high-energy antihydrogen (CERN, Fermilab)
- 2002: creation of 10 K antihydrogen (Athena, Atrap)
- 2011: antihydrogen confinement (Alpha)
- 2013: preliminary Hbar gravity measurement (Alpha)
- 2013: first Hbar beam (Asacusa)

Cold Neutral Antimatter

Future: study of Antimatter properties !!

Study of fundamental Laws with Antimatter at CERN

Marco Giammarchi

Istituto Nazionale Fisica Nucleare - Milano

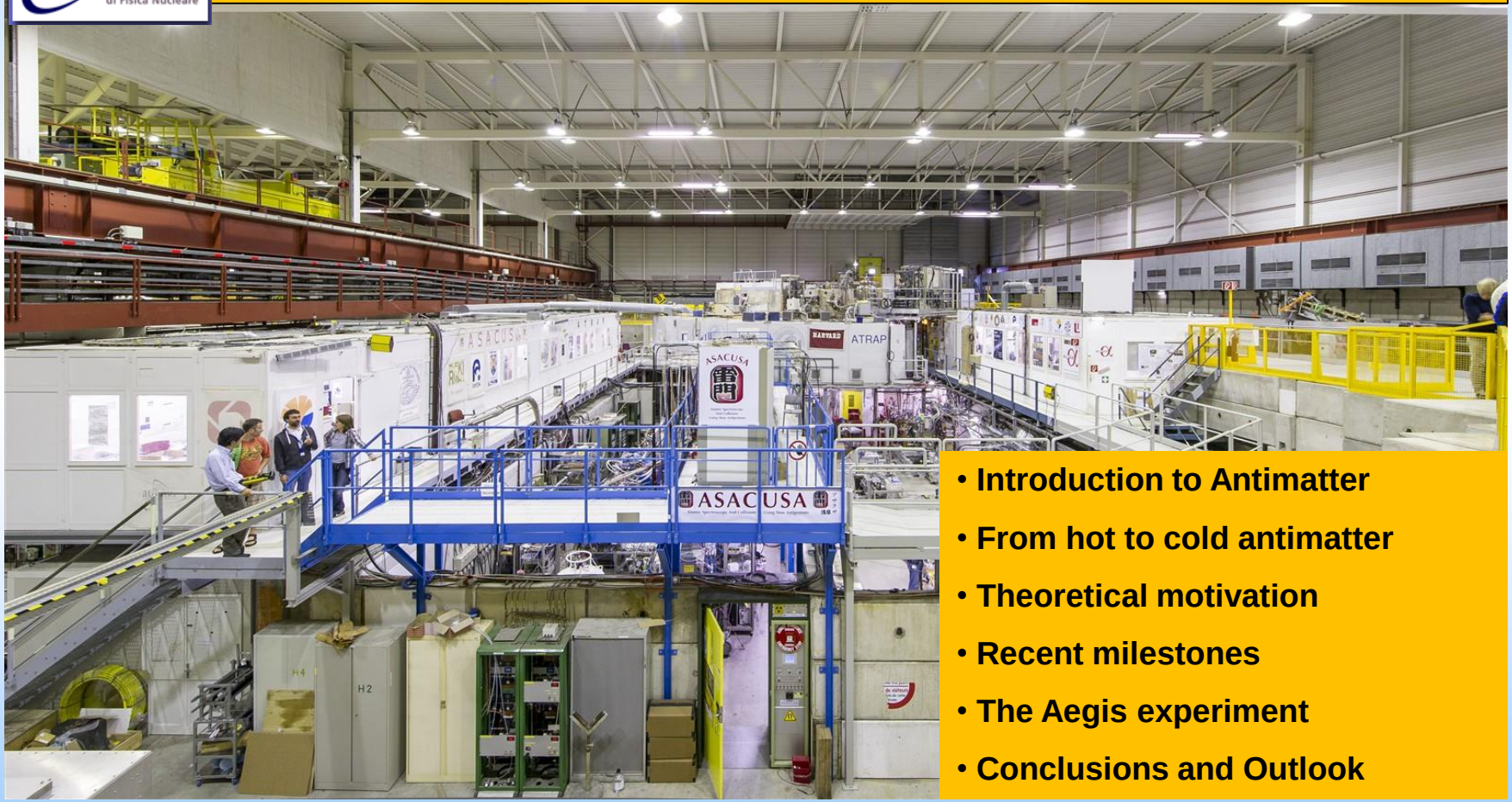

- **Introduction to Antimatter**
- **From hot to cold antimatter**
- **Theoretical motivation**
- **Recent milestones**
- **The Aegis experiment**
- **Conclusions and Outlook**

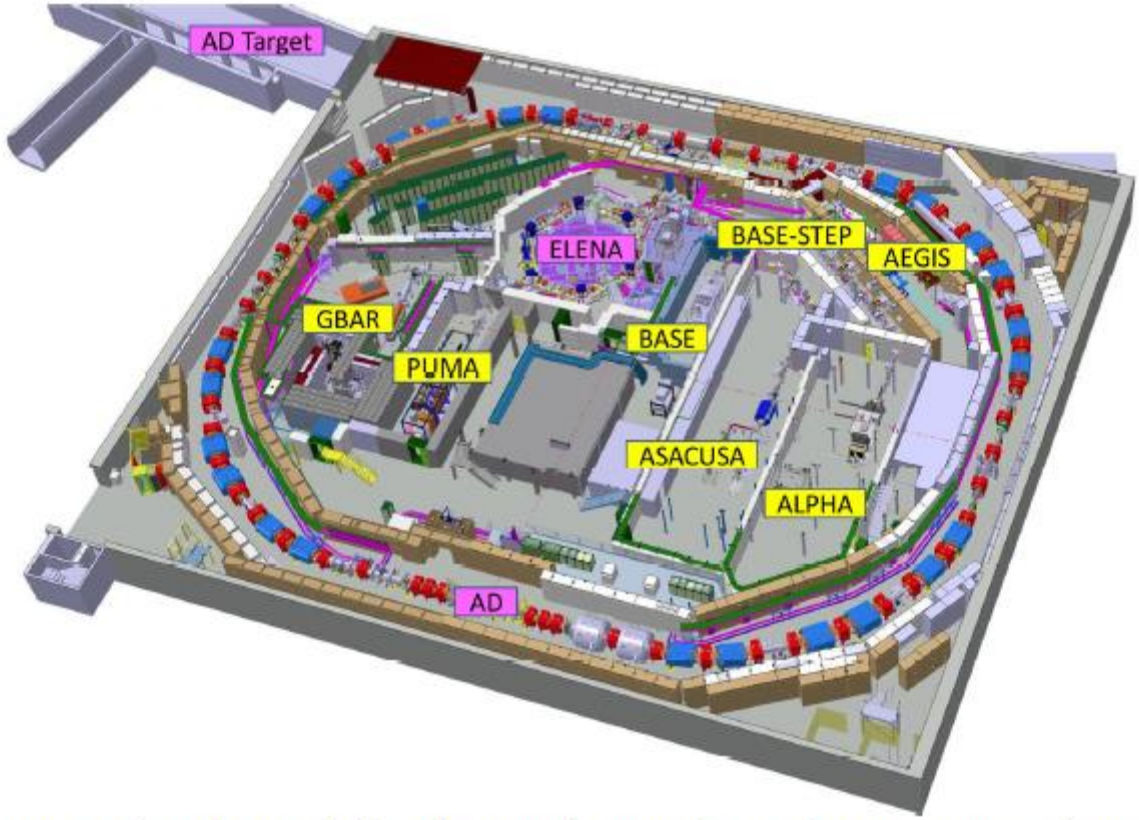

Figure 2. *Overview on the AD/ELENA facility. The AD, with a circumference of 183 m, constrains the area within which ELENA and the experimental areas are located.*

Pure Electron Plasmas

FP II 1/- 2018

Fajans Group

Department of Physics

University of California

Berkeley

REVIEW OF SCIENTIFIC INSTRUMENTS VOLUME 70, NUMBER 12 DECEMBER 1999

Photocathode source for studying two-dimensional fluid phenomena with magnetized electron columns

D. Durkin[a] and J. Fajans
Department of Physics, University of California, Berkeley, Berkeley, California 94720-7300

(Received 28 May 1999; accepted for publication 2 September 1999)

Magnetized electron columns are a valuable experimental tool used to study two-dimensional (2D) fluid phenomena. Traditionally, the electrons have been generated with thermionic sources, typically limiting the initial electron distribution to one filled circle and thereby restricting the range of accessible fluid phenomena. Here, we describe a new electron source based on a cesium antimonide photocathode that can generate more complicated initial electron distributions. Experiments so far have focused on the stability of 2D vortex patterns. © *1999 American Institute of Physics.* [S0034-6748(99)02612-X]

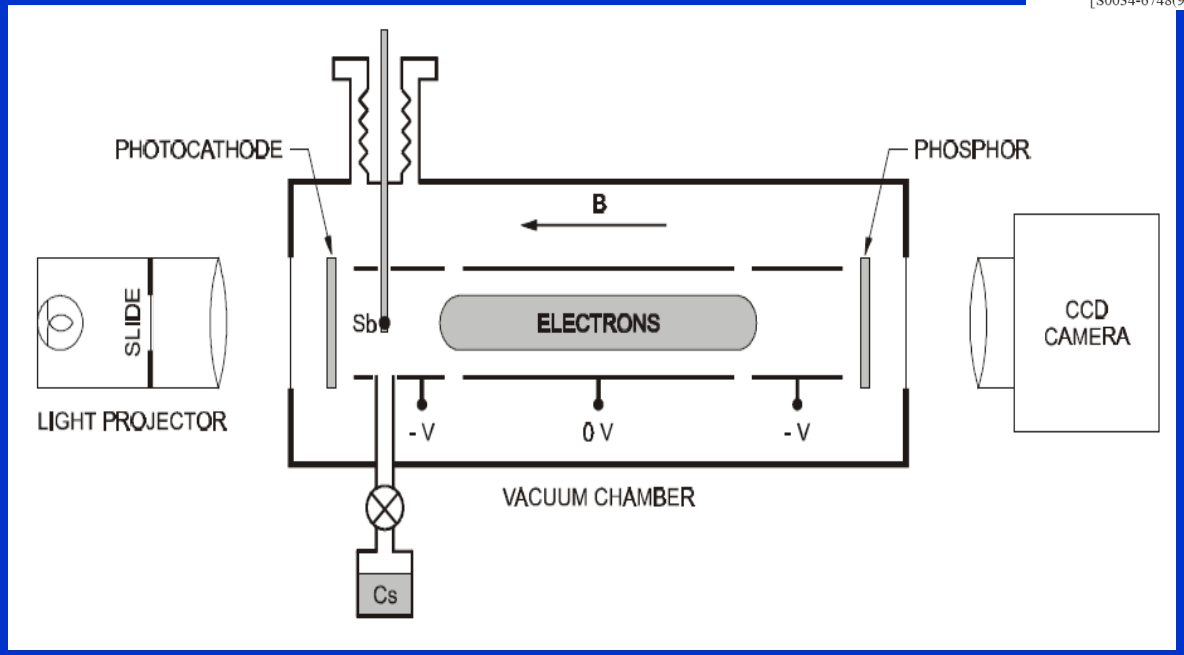

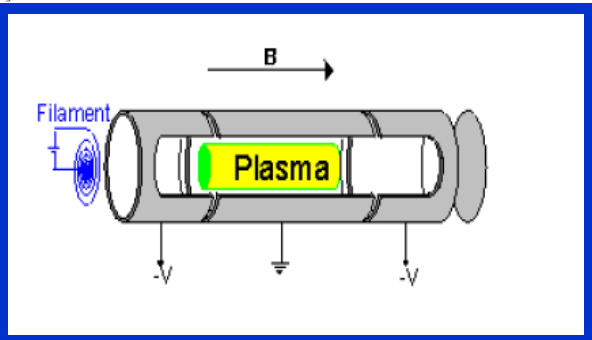

FIG. 1. The geometry of a simple Malmberg-Penning **(M-P)** trap with a photocathode electron source and phosphor screen diagnostic. The antimony (Sb) evaporator and cesium (Cs) source are used to fabricate the photocathode.

Pure electron plasma in M-P trap

FP II 1- 2018

Malmberg-Penning

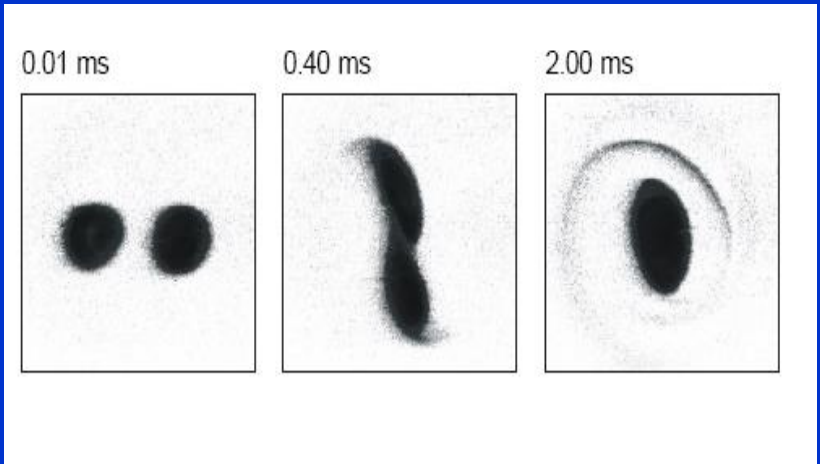

FIG. 2. The evolution of two merging columns.

0.01 ms 0.50 ms 1.00 ms

The photocathode can inject circular electron columns up to several Debye lengths in radius, with densities of 3×10^7 cm^{-3} and temperatures of 3 eV, corresponding to Debye lengths of approximately 0.2 cm (these values depend on the light source's intensity, the cathode's voltage, and the photocathode's quantum efficiency). Unlike thermionic sources, it cannot inject columns many Debye lengths in radius. An option to facilitate this is presented in Sec. IV. The photocathode's advantage over thermionic sources is its ability to inject more complicated distributions, as illustrated by the following examples:

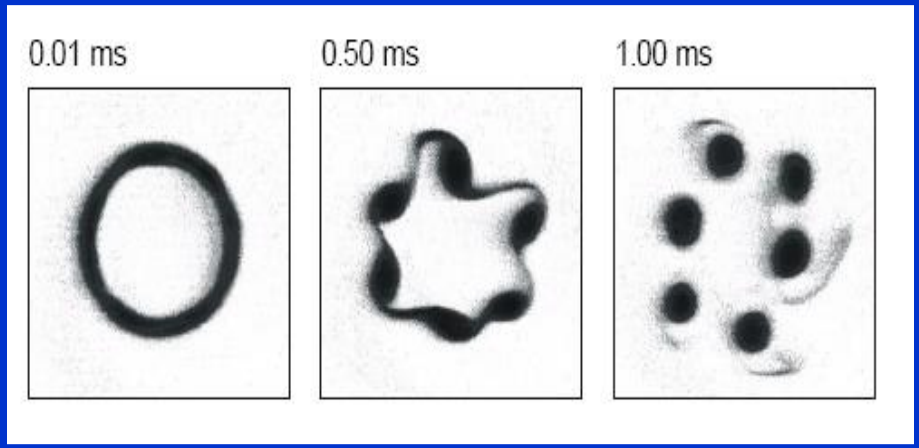

FIG. 3. The evolution of a hollow column by the Diocotron instability.

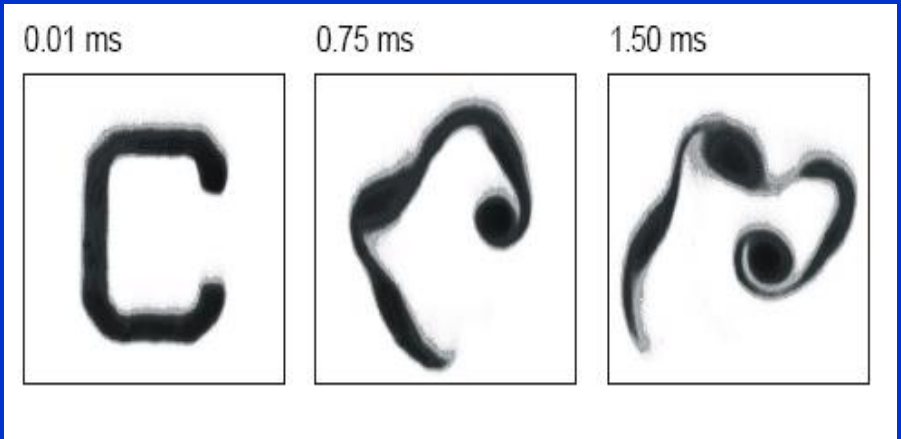

The photocathode can inject circular electron columns up to several Debye lengths in radius, with densities of 3×10^7 cm^{-3} and temperatures of 3 eV, corresponding to Debye lengths of approximately 0.2 cm (these values depend on the light source's intensity, the cathode's voltage, and the photocathode's quantum efficiency). Unlike thermionic sources, it cannot inject columns many Debye lengths in radius. An option to facilitate this is presented in Sec. IV. The photocathode's advantage over thermionic sources is its ability to inject more complicated distributions, as illustrated by the following examples:

FIG. 5. The \Go Bears!" evolution.

Gabrielse

Method 1: Nested Penning Trap

3-Body "Recombination"

Volume 129, number 1 PHYSICS LETTERS A 2 May 1988

ANTIHYDROGEN PRODUCTION USING TRAPPED PLASMAS

G. GABRIELSE, S.L. ROLSTON, L. HAARSMA
Department of Physics, Harvard University, Cambridge, MA 02138, USA

and

W. KELLS
Fermi National Accelerator Laboratory, Batavia, IL 60438, USA

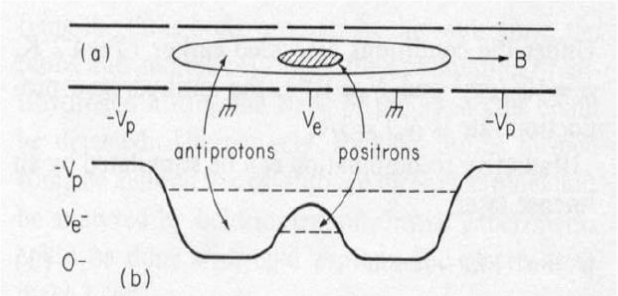

Fig. 1. Electrodes (a) and axial potential (b) for a nested pair of Penning traps.

Nested Penning Trap

We call attention to another three-body recombination

$$p^- + e^+ + e^+ \rightarrow \bar{H} + e^+ , \quad (6)$$

which may well be more efficient for antihydrogen production by many orders of magnitude. Its cross

3-Body "Recombination"

Malmberg - Penning trap

- Production of Antihydrogen
- Antihydrogen confinement

Available online at www.sciencedirect.com
SCIENCE DIRECT®
ELSEVIER
Nuclear Instruments and Methods in Physics Research A 521 (2004) 318–325
NUCLEAR INSTRUMENTS & METHODS IN PHYSICS RESEARCH Section A
www.elsevier.com/locate/nima

Malmberg–Penning and Minimum-B trap compatibility: the advantages of higher-order multipole traps ☆

J. Fajans*, A. Schmidt
Department of Physics, University of California, 366 LeConte Hall, Berkeley, CA 94720, USA

Received 16 June 2003; received in revised form 21 October 2003; accepted 7 November 2003

Table 1
Approximate ATHENA and ATRAP System Parameters [21,22]

	ATHENA	ATRAP
Temperature	15 K	4.2 K
Solenoidal field	3 T	5.4 T
Positron density	2×10^8 cm^{-3}	1×10^8 cm^{-3}
Positron column length	3.2 cm	0.8 cm
Positron Debye length	0.0019 cm	0.0014 cm
Anti-proton density	10^4 cm^{-3}	10^4 cm^{-3}
Anti-proton column length	1.0 cm	1.0 cm
Anti-proton Debye length	0.27 cm	0.14 cm

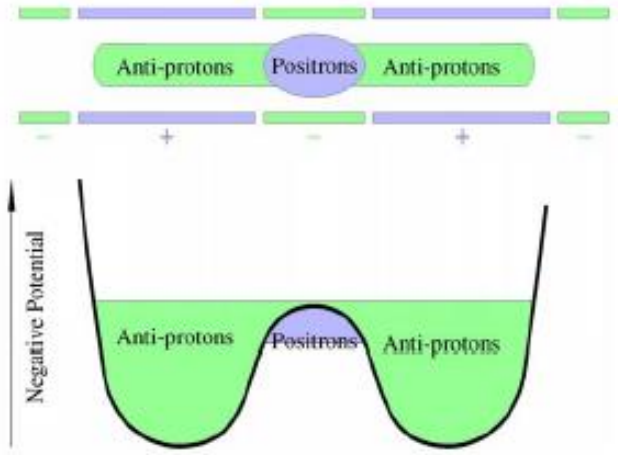

Fig. 1. Schematic diagram showing a double-well Malmberg–Penning trap similar to those used by ATHENA and ATRAP.

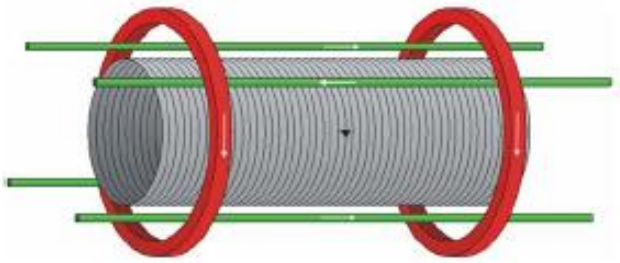

Fig. 2. The field coils for a quadrupole Minimum-B/Malmberg–Penning trap. (The electrostatic structures shown in Fig. 1 are placed inside the solenoid.) The solenoid produces the axial field for the Penning–Malmberg trap, the two end coils generate the mirror field that confines $\bar{H}$ axially, and the four quadrupole wires generate the field that confines $\bar{H}$ radially. This configuration is similar to a Joffe configuration. To trap $\bar{H}$, the mirror coils must be positioned so that the minimum in the field extends over the overlap region in Fig. 1. Because the coils induce transport, they may need to be pushed far enough away that their field is small over the entire plasma region.

Antimatter trap

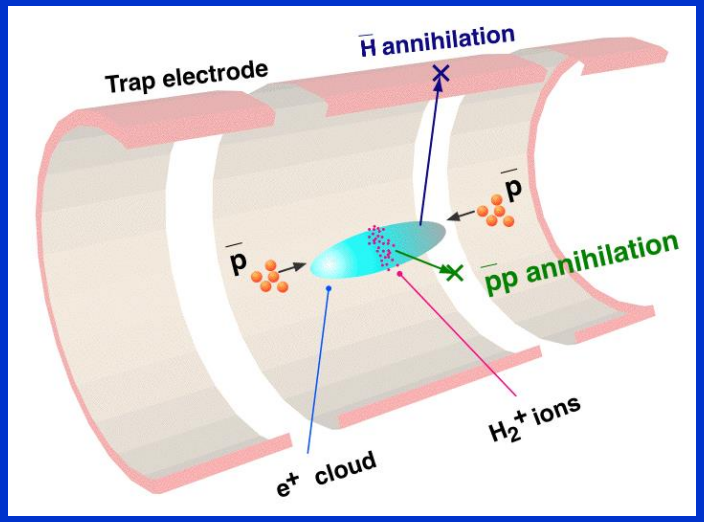

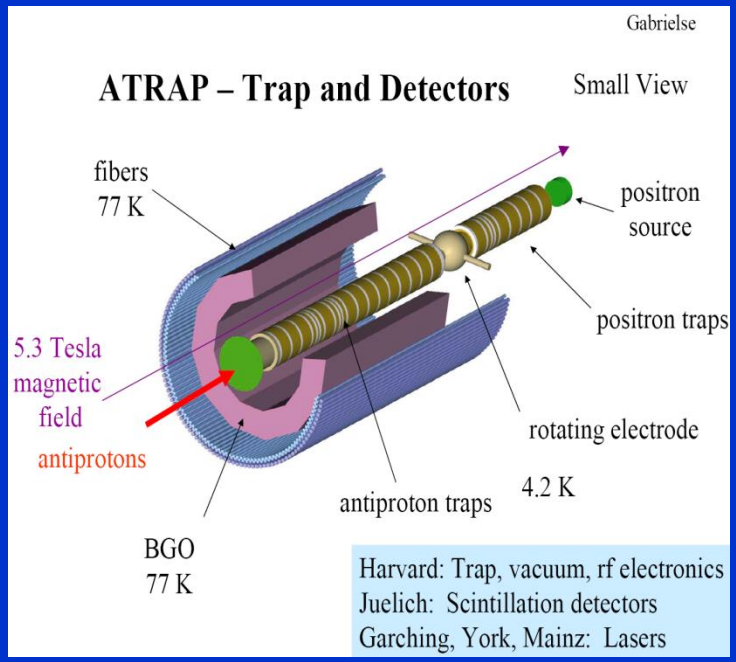

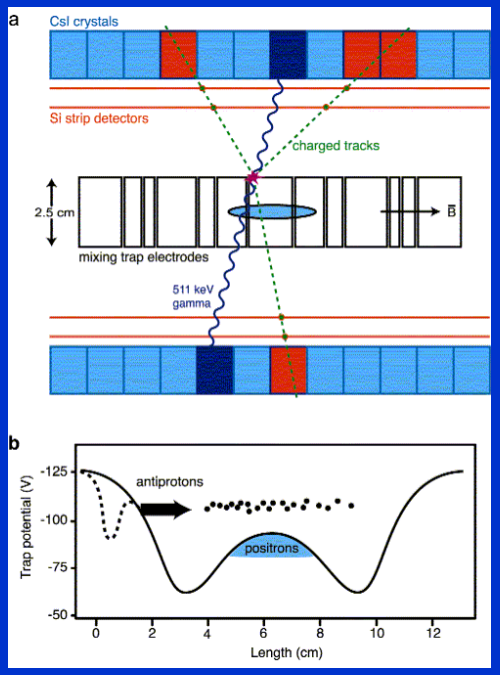

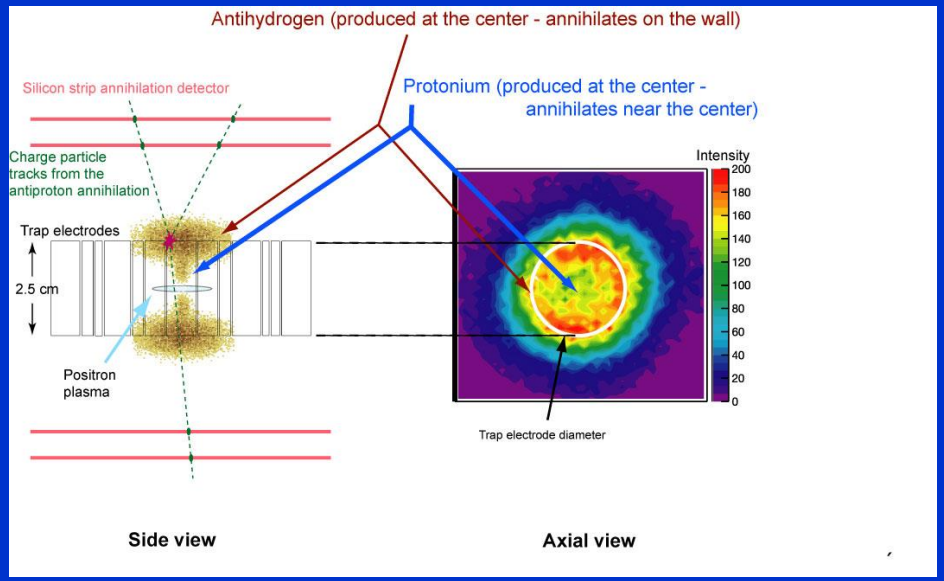

ATRAP

Gabrielse

ATRAP – Trap and Detectors

Small View

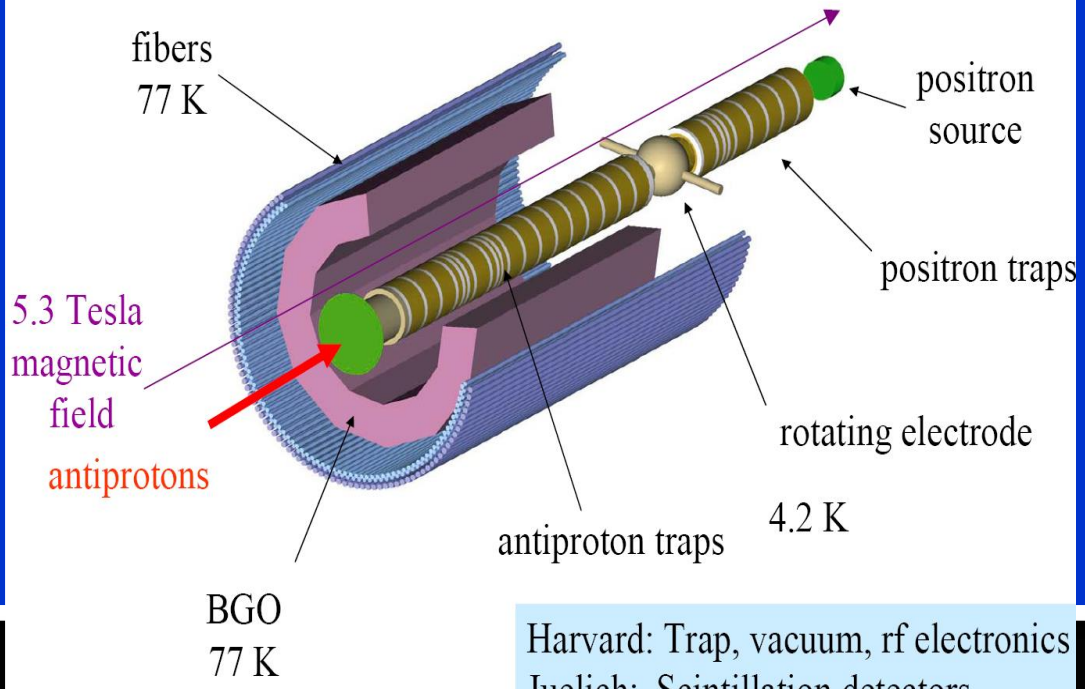

Harvard: Trap, vacuum, rf electronics
Juelich: Scintillation detectors
Garching, York, Mainz: Lasers

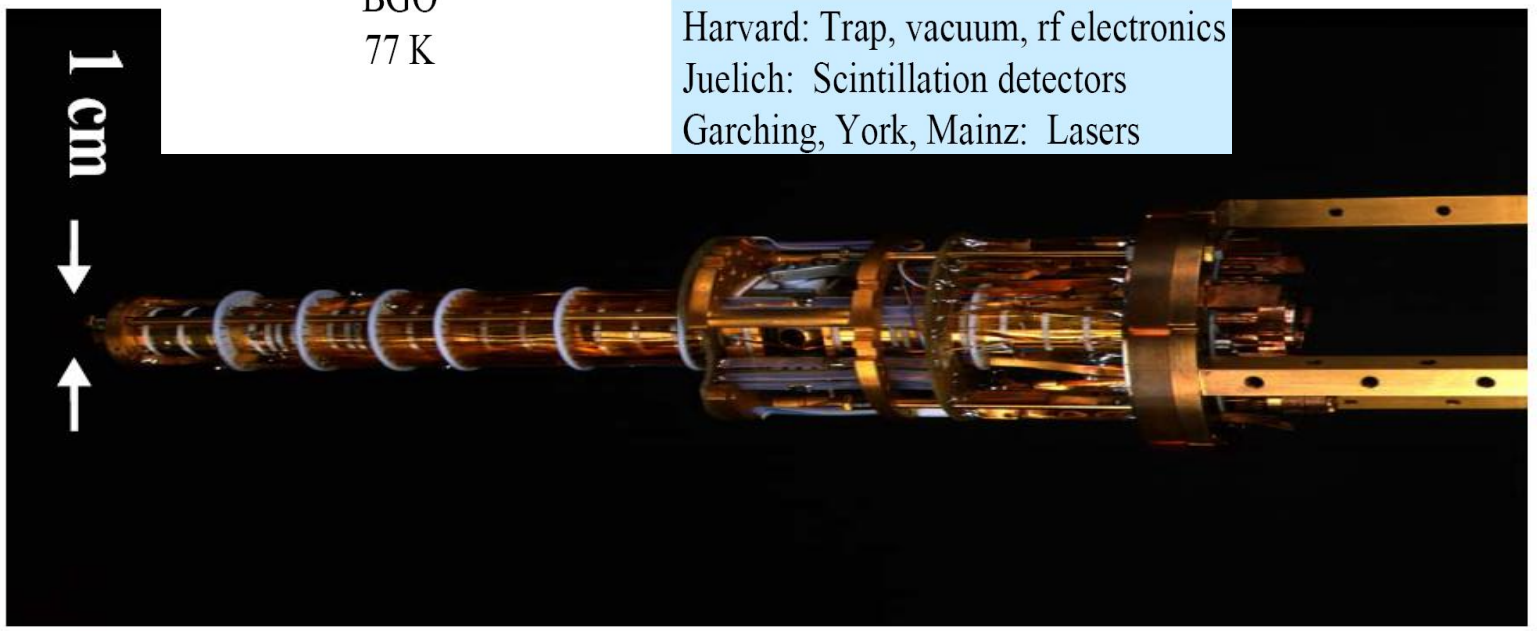

The latest news from ATHENA

FP II 1- 2018

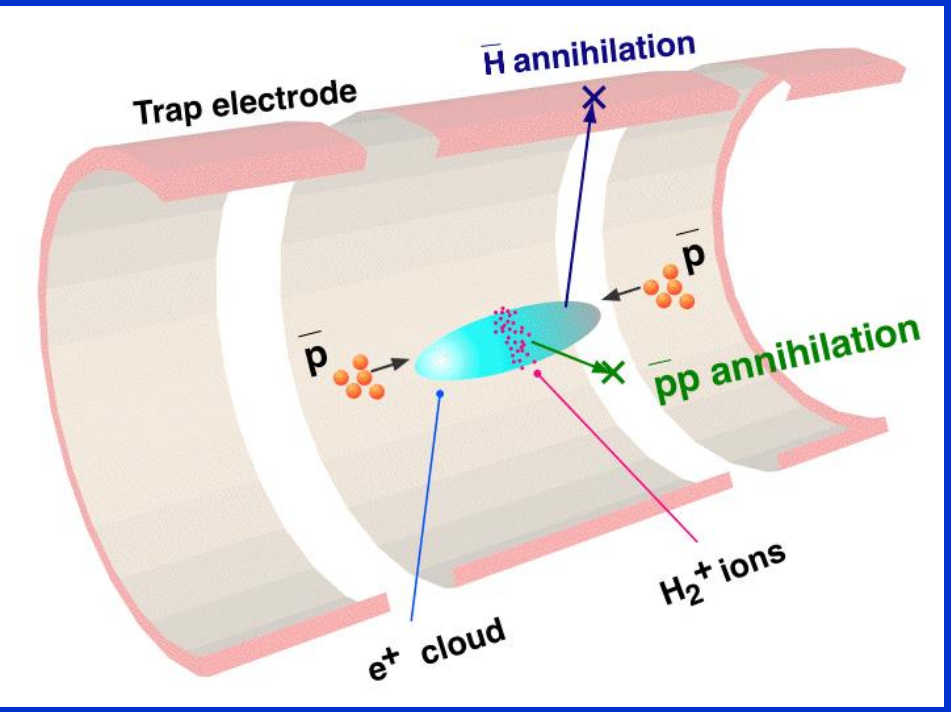

November 22, 2006

ATHENA publishes results on laser stimulated formation of antihydrogen atoms.

October 9, 2006

ATHENA publishes evidence for the first formation of slow antiprotonic hydrogen (protonium) – the first antimatter chemistry.

PRL 108, 113002 (2012) PHYSICAL REVIEW LETTERS week ending 16 MARCH 2012

Trapped Antihydrogen in Its Ground State

G. Gabrielse,[1,*] R. Kalra,[1] W. S. Kolthammer,[1] R. McConnell,[1] P. Richerme,[1] D. Grzonka,[2] W. Oelert,[2] T. Sefzick,[2] M. Zielinski,[2] D. W. Fitzakerley,[3] M. C. George,[3] E. A. Hessels,[3] C. H. Storry,[3] M. Weel,[3] A. Müllers,[4] and J. Walz[4]

(ATRAP Collaboration)

Antihydrogen atoms ($\bar{H}$) are confined in an Ioffe trap for 15–1000 s—long enough to ensure that they reach their ground state. Though reproducibility challenges remain in making large numbers of cold antiprotons ($\bar{p}$) and positrons (e^+) interact, 5 ± 1 simultaneously confined ground-state atoms are produced and observed on average, substantially more than previously reported. Increases in the number of simultaneously trapped $\bar{H}$ are critical if laser cooling of trapped $\bar{H}$ is to be demonstrated and spectroscopic studies at interesting levels of precision are to be carried out.

Gabrielse

LEAR – Low Energy Antiproton Ring

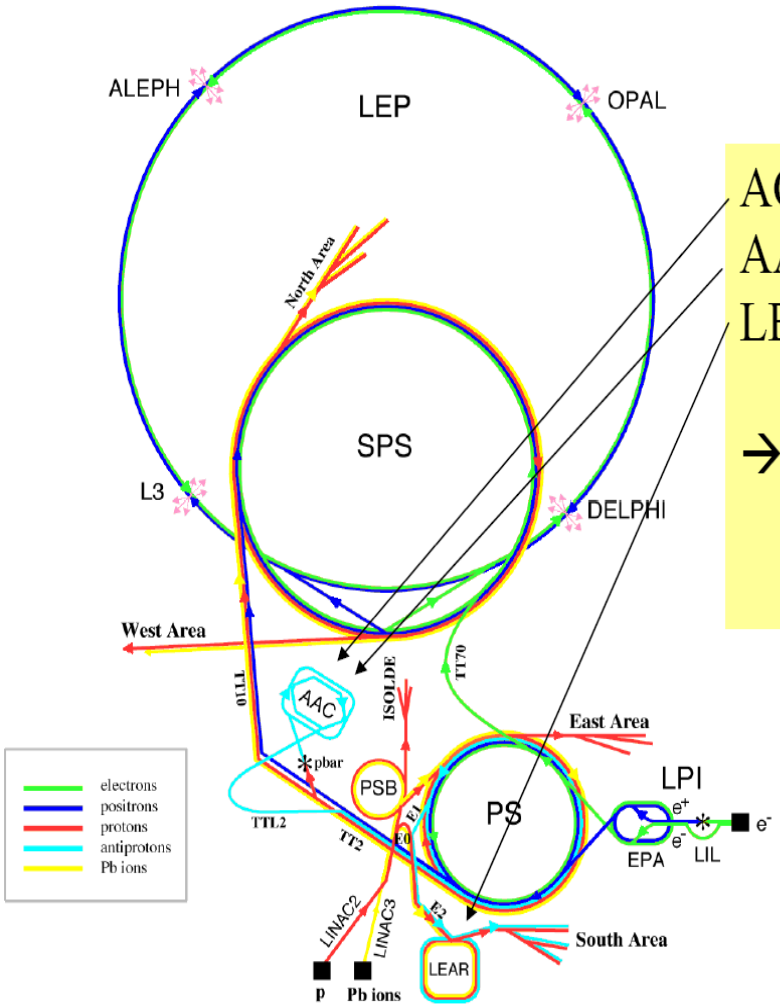

AC – catch antiprotons
AA – stack antiprotons, cool
LEAR – decelerate antiprotons

→We got 10^9 antiprotons
in a pulse every 5 minutes
(maximum, need refill time)

Antiprotons: CERN's "Accelerators"

Swansea University
Prifysgol Abertawe

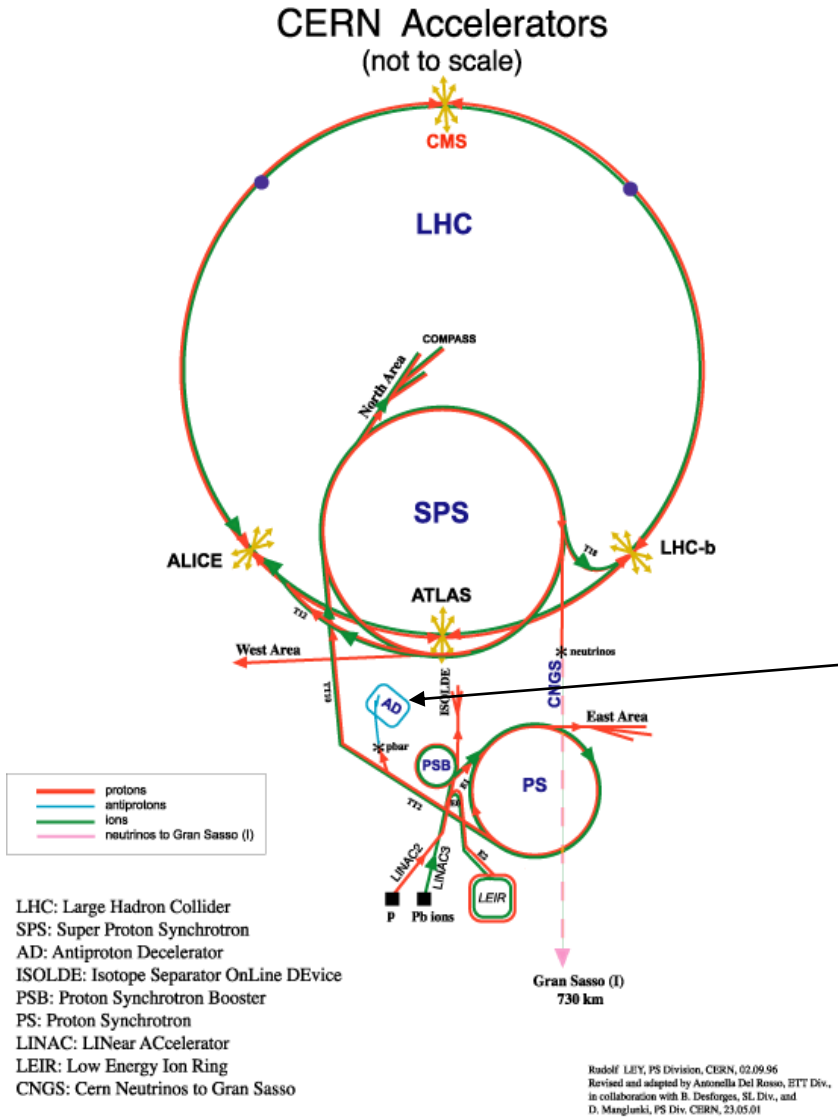

The Antiproton Decelerator

Antiprotons: the AD, Antiproton Decelerator

Swansea University
Prifysgol Abertawe

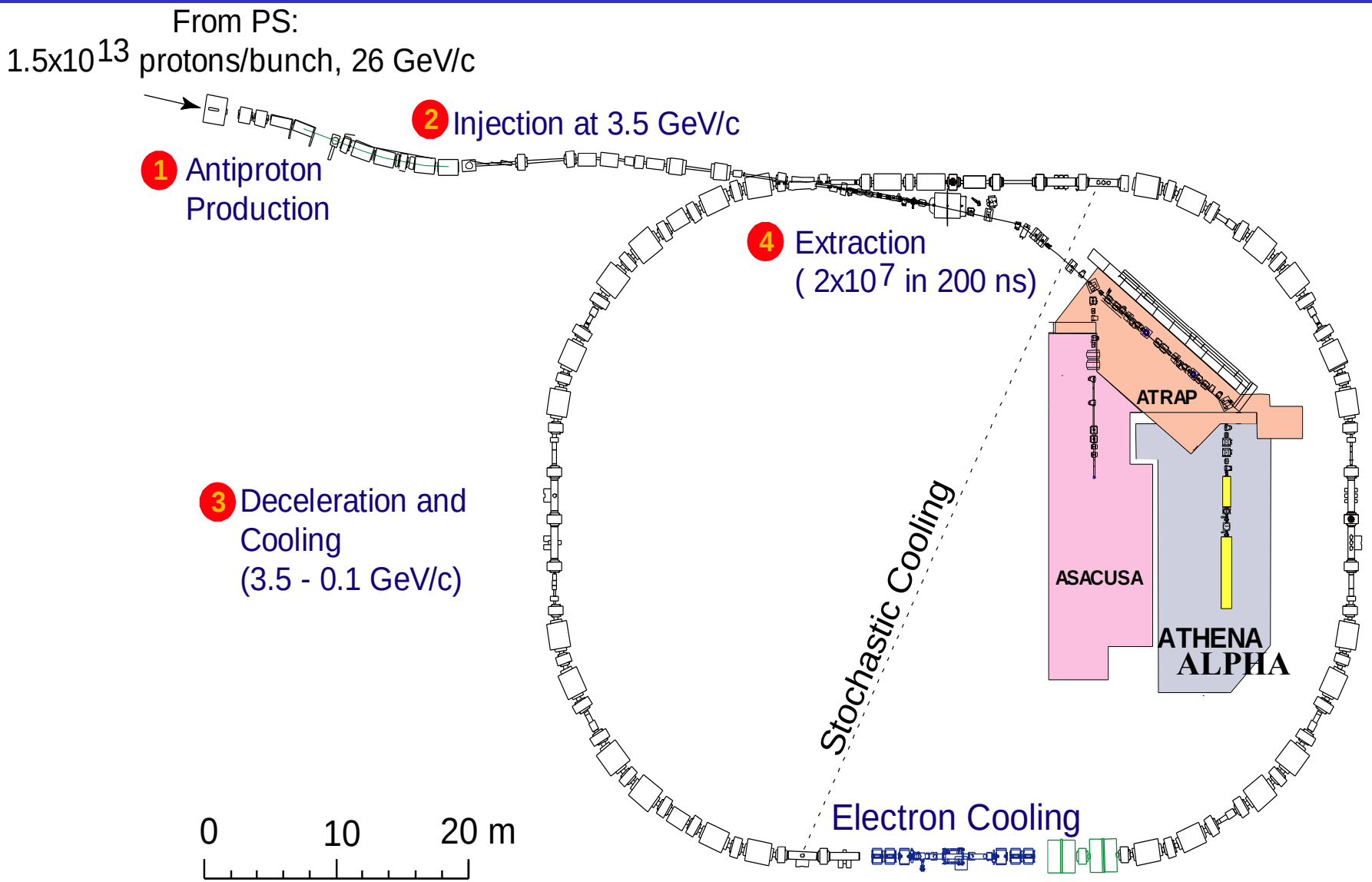

ALPHA: An Antihydrogen Trapping Experiment

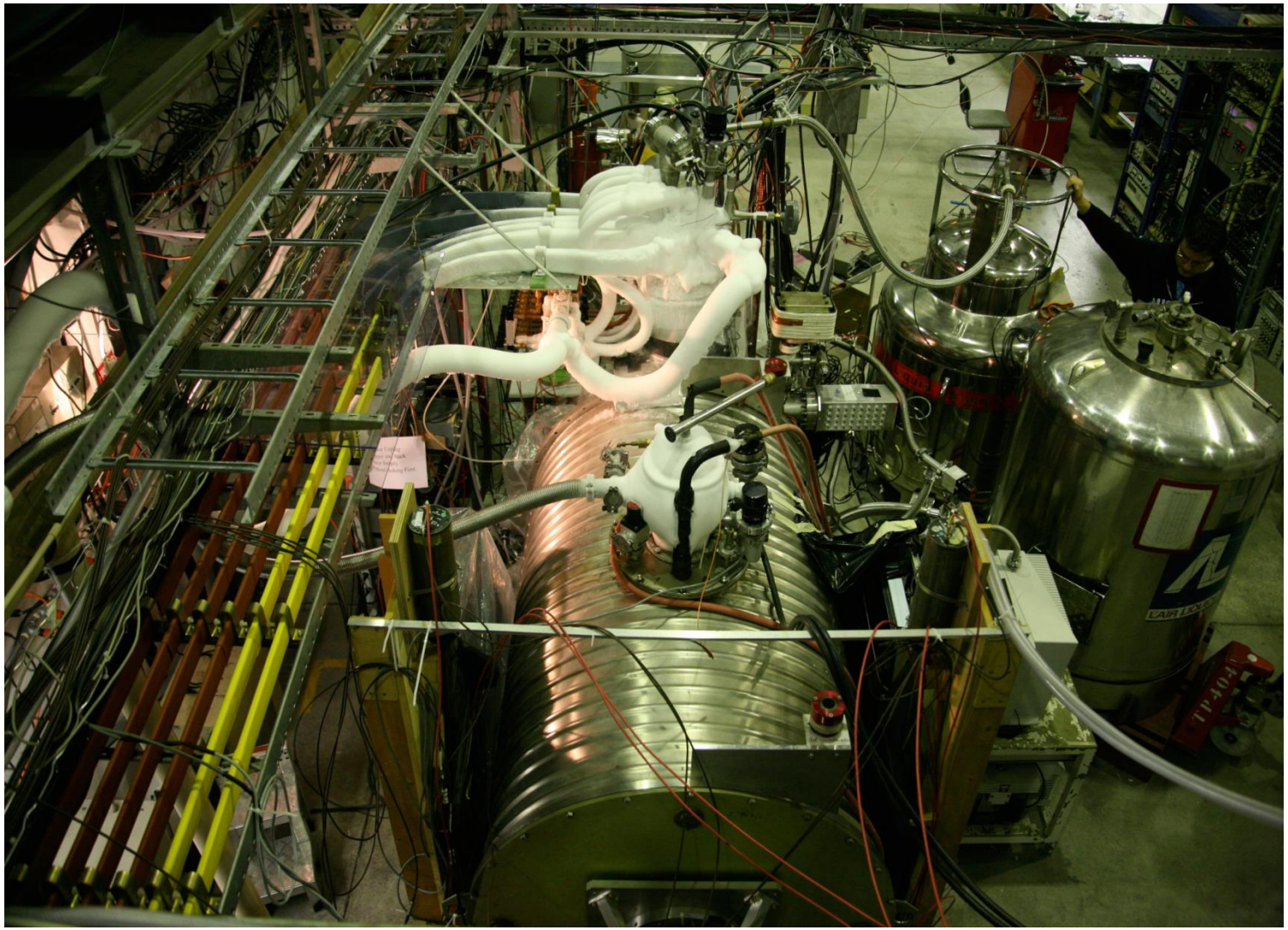

Antiprotons: Capture and Cooling

Swansea University
Prifysgol Abertawe

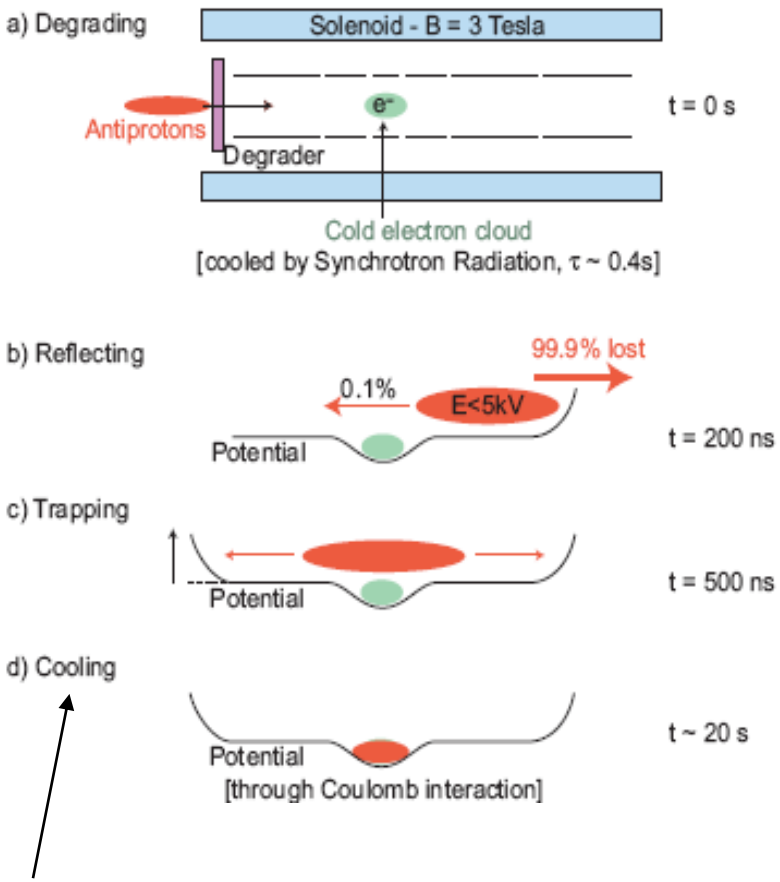

To (or close to) the trap temperature

The trap walls were cooled to 15 K

ATHENA

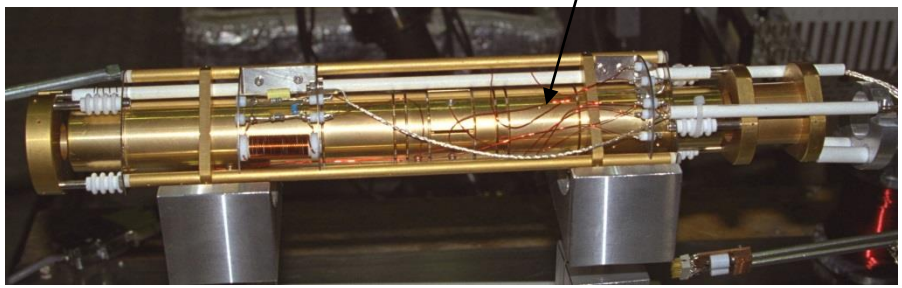

Antiproton Capture Trap

Similar apparatus used currently in ALPHA; method originally devised by Gabrielse and co-workers (PRL, 63, 1360 (1989))

ATHENA

FP II 1- 2018

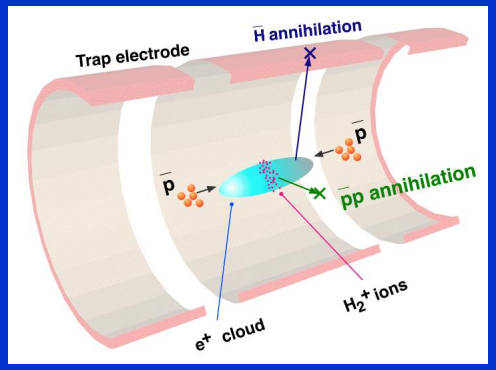

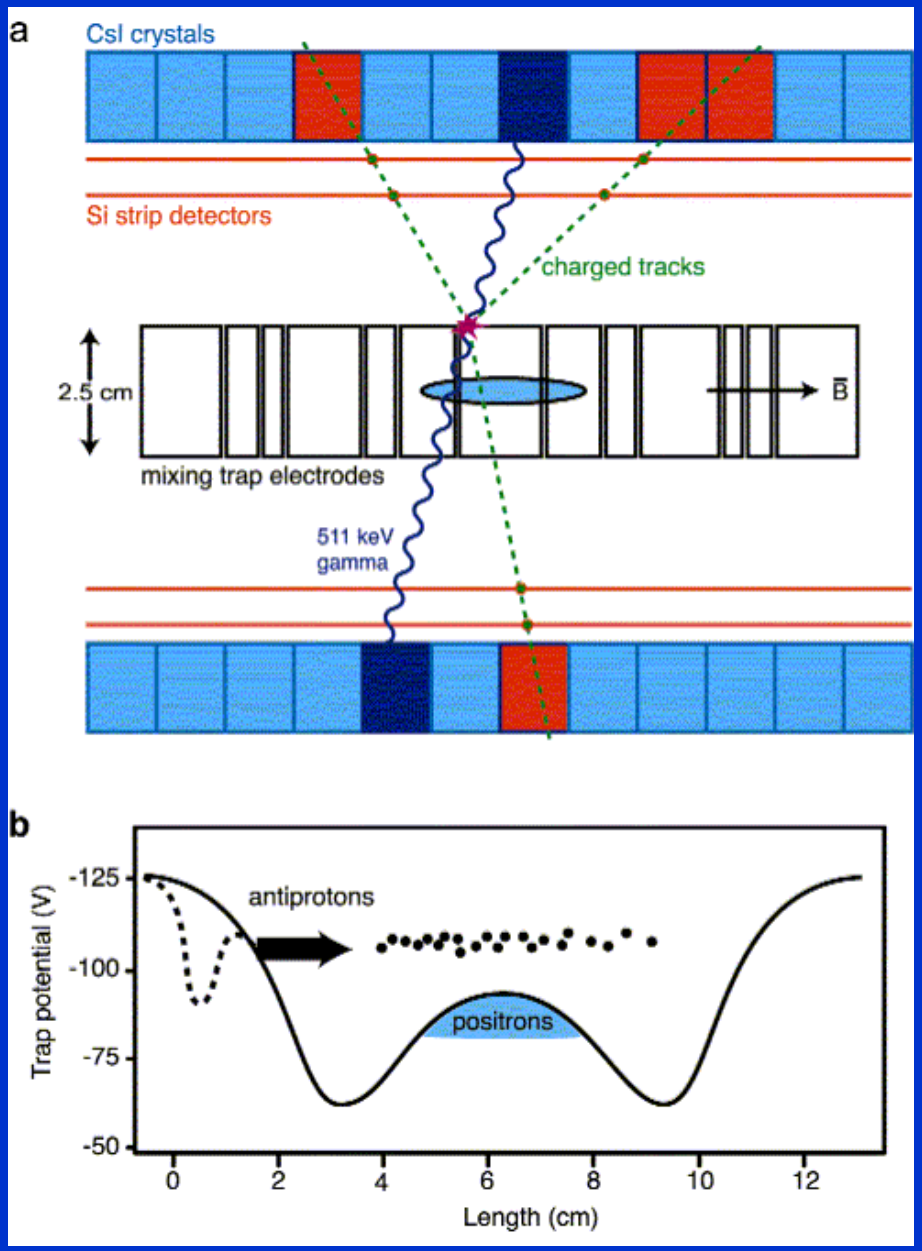

Figure 1 Central part of the ATHENA apparatus and trapping potential.
a, Schematic diagram, in axial section, of the ATHENA mixing trap and antihydrogen detector. The cylindrical electrodes and the position of the positron cloud (blue ellipse) are shown. A typical antihydrogen annihilation into three charged pions and two back-to-back 511-keV photons is also shown. The arrow indicates the direction of the magnetic field. The detector active volume is 16 cm long and has inner and outer diameters of 7.5 cm and 14 cm, respectively.
b, The trapping potential is plotted against length along the trap. The dashed line is the potential immediately before antiproton transfer. The solid line is the potential during mixing.

Slow antiprotonic hydrogen (protonium FP II 1- 2018

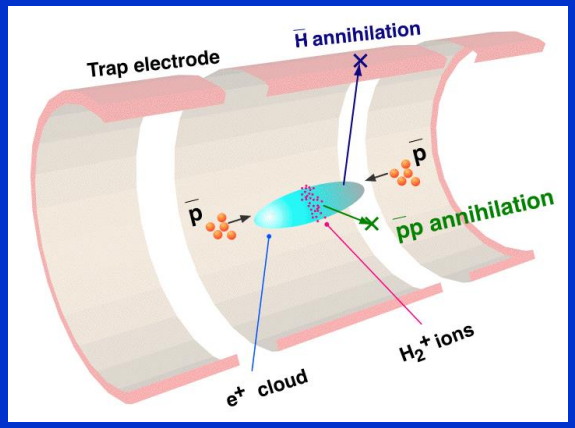

October 9, 2006 ATHENA

first formation of slow antiprotonic hydrogen (protonium) –

the first antimatter chemistry.

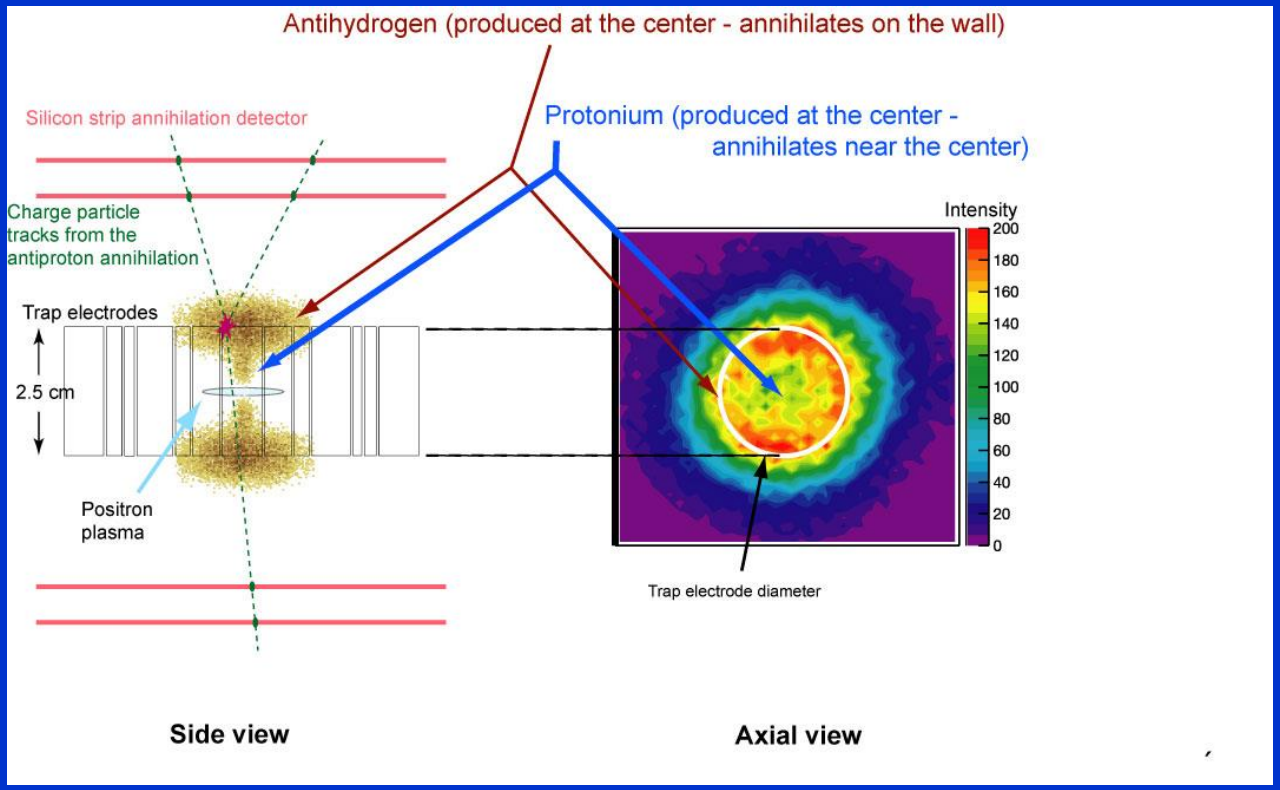

Antihydrogen is formed all along the positron plasma and lives long enough to annihilate on the wall. Protonium is formed mainly at the center of the positron plasma where the molecular hydrogen ions are concentrated and does not live long enough to annihilate on the wall, but instead annihilates in flight towards the wall.

The ATHENA experiment

Cold Antihydrogen

FP II 1- 2018

The ATHENA experiment takes a completely different approach to producing antihydrogen. The idea is to produce antihydrogen atoms at low energy – essentially at rest – in order to be able to study their properties. The AD machine at CERN was built to take antiprotons, which are produced in high-energy collisions, and decelerate them to more manageable energies.

The ATHENA apparatus slows, cools, and traps antiprotons from the AD. The antiprotons are trapped in high vacuum in an electromagnetic 'bottle' known as a Penning trap. At the same time, positrons from a radioactive source are accumulated in another trap. The two clouds of charged particles (about 10000 antiprotons and 70 million positrons) are mixed together to produce antihydrogen. All of this takes place in a cryogenic environment at about 15 degrees above absolute zero.

Antihydrogen atoms that are formed escape the electromagnetic trap because they have no net charge. They then annihilate and are detected by a specially built detector, unique to the ATHENA experiment. Antihydrogen produces a very characteristic annihilation signal in this detector, allowing researchers to confirm its production.

To date, ATHENA has directly detected 131±22 atoms of antihydrogen. This implies that about 50.000 anti-atoms were actually produced in the apparatus, since most of them escape detection.

The next step for ATHENA is to try to make measurements of the spectrum of antihydrogen and try to compare these to hydrogen. Any difference in these two spectra would require fundamental changes to our current model of matter and antimatter. These experiments could begin as early as next year, when the AD physics program resumes in May.

The ATHENA result is a significant milestone in antimatter science, and it opens the door to the anticipated application of modern techniques of atom trapping, cooling, and manipulation to the realm of atomic antimatter. Tests of the behaviour of antimatter under the influence of gravity are also an interesting future perspective.

Background

Background

Nature, as far as we know, consists of normal matter – atoms such as hydrogen and carbon, which in turn contain positively charged protons, uncharged neutrons and negatively charged electrons. However, physicists have known since the 1930's that for each of the particle types of normal matter, there exists an equivalent particle of antimatter. Antimatter particles should have the same mass, but opposite charge, as their matter counterparts. Matter and antimatter don't like to co-exist; if a particle meets its antiparticle, they annihilate in a burst of energy – often creating new particle-antiparticle pairs. The energy release during matter-antimatter annihilation is often the basis for futuristic propulsion schemes in popular science fiction literature, such as Star Trek. Cosmologists believe that there were equal amounts of matter and antimatter at the beginning of the Universe – the so-called Big Bang. Why the universe is now composed of matter is a topic of great interest in theoretical physics. According to the laws of physics as we understand them today, it should be possible to build a universe containing only antimatter.

The laws of physics that govern the interactions of fundamental particles are often collectively referred to as The Standard Model. The Standard Model places some restrictive conditions on the relationship between matter and antimatter. Thus, comparing the characteristics of matter and antimatter serves to test the underlying theory of the Standard Model. Essential to the Standard Model is the so-called CPT theorem, which involves discrete symmetries. The CPT theorem requires that the laws of physics be invariant under the following operation: all particles are replaced by their antiparticle counterparts (Charge conjugation), all spatial coordinates are reflected about the origin (Parity), and the flow of time is reversed (Time reversal). The CPT theorem has important implications for antimatter, including the above-mentioned mass equivalence of particle and antiparticle.

The CPT theorem also requires that atoms and their anti-atom equivalents behave in the same way. For example, hydrogen and antihydrogen should have the same spectrum – the frequencies or colours of light that they emit and absorb. It has long been a goal of physicists to be able to produce atoms of anti-hydrogen, in order to compare their spectra with that of hydrogen. An antihydrogen atom consists of an antiproton (negatively charged) and a positron (the antimatter counterpart to the electron). Antihydrogen atoms were first reported to be observed at CERN in 1996 and at Fermilab (near Chicago in the USA) in 1998, but these experiments produced very few antihydrogen atoms, and these at velocities close to the speed of light. The antihydrogen lived for a very short time before colliding with normal matter and annihilating. There was no possibility for making precision comparison measurements of hydrogen and antihydrogen in these experiments, which only demonstrated the existence of antihydrogen.

http://home.cern/topics/antimatter

Physicists from CERN's Atomic Spectroscopy and Collisions Using Slow Antiprotons (ASACUSA) project say they have produced at least 80 atoms of antihydrogen.

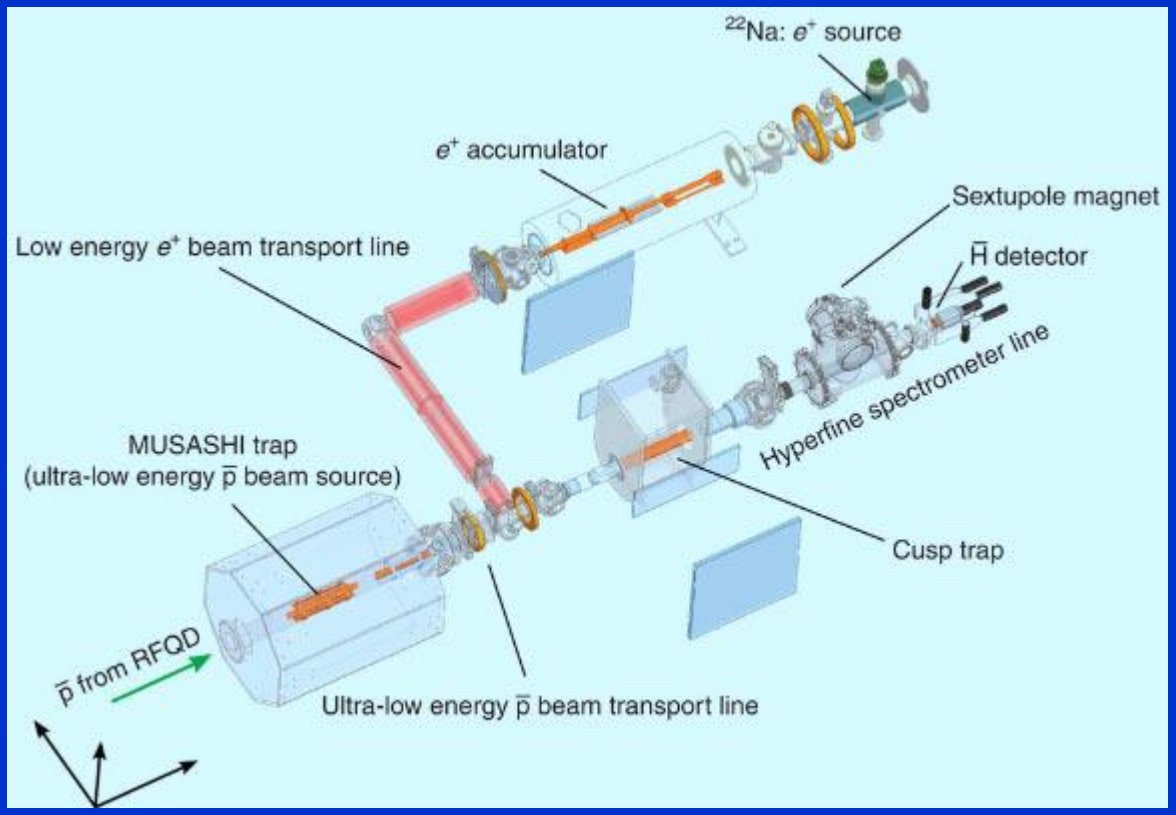

Schematic view of ASACUSA's experimental apparatus. Antiprotons delivered from the antiproton decelerator via the radio-frequency quadrupole decelerator (RFQD) are trapped, electron-cooled and radially compressed in an ultra-slow antiproton beam source, named MUSASHI. Moderated positrons from a 22Na source are prepared and cooled in the positron accumulator and then are transported to the cusp trap. The cusp trap consists of multiple ring electrodes and superconducting anti-Helmholtz coils. After positrons are accumulated near the maximum magnetic field region, antiprotons are injected from the MUSASHI and mixed with positrons synthesizing antihydrogen atoms. Antihydrogen atoms in low-field-seeking states are focused downstream of the cusp trap due to the strong magnetic field gradient, while those high-field-seeking states are de-focused. Thus, a polarized antihydrogen beam is produced. Image credit: Kuroda N et al.

Kuroda N et al. 2014. A source of antihydrogen for in-flight hyperfine spectroscopy. *Nature Communications* 5, article number: 3089; doi: 10.1038/ncomms4089

First Antihydrogen Beam

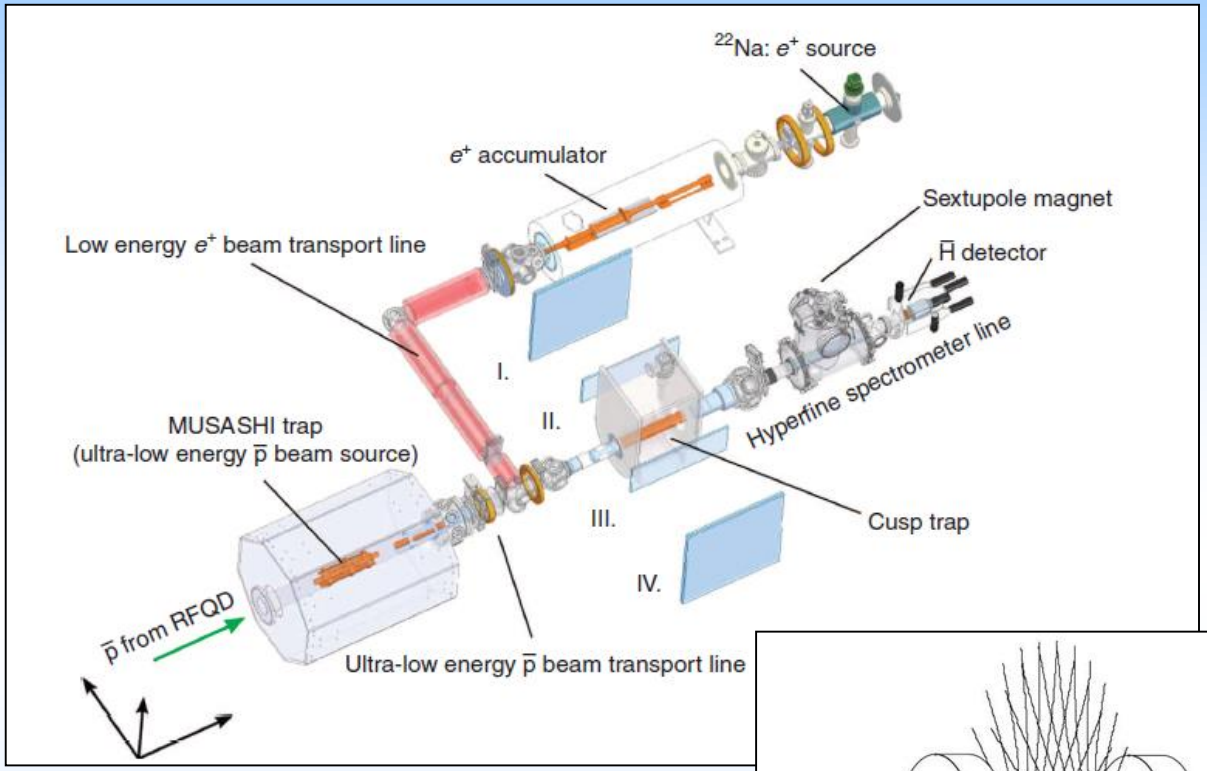

ASACUSA
N.Kuroda et al.
Nature Communications
DOI 10.1038/ncomms4089

Production and storage of positrons in the CUSP trap

Injection of antiprotons in the CUSP trap

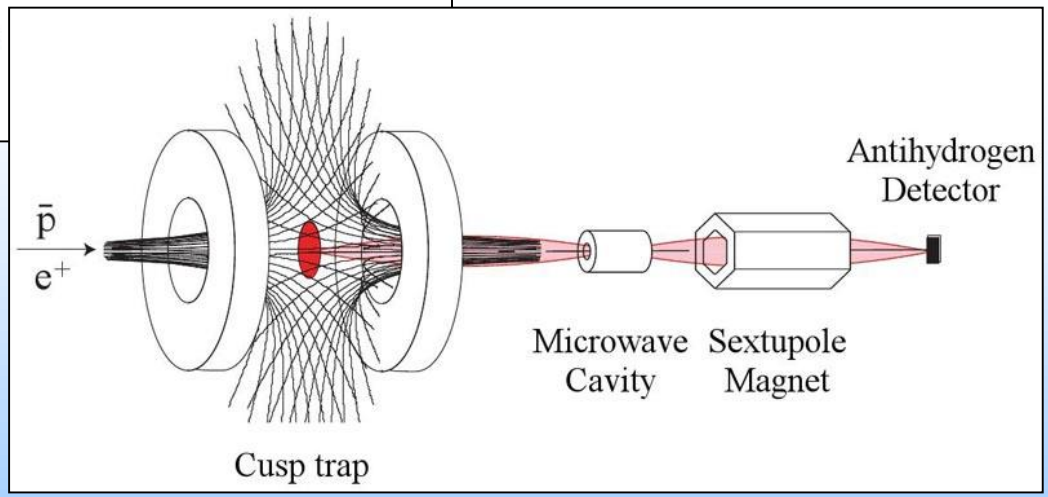

Detection of Antihydrogen 2.7 m downstream in a magnetic field free environment

1995

FP II - 2018

First antiatoms produced: antihydrogen, at CERN

A team led by Walter Oelert created atoms of antihydrogen for the first time at CERN's Low Energy Antiproton Ring (LEAR) facility. Nine of these atoms were produced in collisions between antiprotons and xenon atoms over a period of 3 weeks. Each one remained in existence for about 40 billionths of a second, travelled at nearly the speed of light over a path of 10 metres and then annihilated with ordinary matter. The annihilation produced the signal that showed that the anti-atoms had been created.

This was the first time that antimatter particles had been brought together to make complete atoms, and the first step in a programme to make detailed measurements of antihydrogen.

The hydrogen atom is the simplest atom of all, made of a single proton orbited by an electron. Some three quarters of all the ordinary matter in the universe is hydrogen, and the hydrogen atom is one of the best understood systems in physics. Comparison with antihydrogen offers a route to understanding the matter–antimatter asymmetry in the universe.

2002

ATHENA and ATRAP create "cold" antimatter

Two CERN experiments, ATHENA and ATRAP, created thousands of atoms of antimatter in a "cold" state in 2002. Cold means that the atoms are slow moving, which makes it possible to study them before they meet ordinary matter and annihilate. Antihydrogen formed in the experiments when cold positrons and antiprotons were brought together and held in a specially designed "trap". Once formed, the electrically neutral antihydrogen atoms drifted out of the trap and annihilated.

2011

ALPHA traps antimatter atoms for 1000 seconds

The ALPHA experiment at CERN reported today that it succeeded in trapping antimatter atoms for over 16 minutes: long enough to begin to study their properties in detail. ALPHA is part of a broad programme at CERN's antiproton decelerator investigating the mysteries of one of nature's most elusive substances.

ALPAH studied 300 trapped antiatoms. Trapping antiatoms will allow antihydrogen to be mapped precisely using laser or microwave spectroscopy so that it can be compared to the hydrogen atom, which is among the best-known systems in physics. Any difference between matter and antimatter should become apparent under careful scrutiny.

CERN

ASACUSA weighs antimatter to one part in a billion

In a paper published today in the journal Nature, the Japanese-European ASACUSA experiment at CERN reported a new measurement of the antiproton's mass accurate to about one part in a billion. Precision measurements of the antiproton mass provide an important way to investigate nature's apparent preference for matter over antimatter.

To make these measurements antiprotons are first trapped inside helium atoms, where they can be 'tickled' with a laser beam. The laser frequency is then tuned until it causes the antiprotons to make a quantum jump within the atoms, and from this frequency the antiproton mass can be calculated. However, an important source of imprecision comes from the fact that the atoms jiggle around, so that those moving towards and away from the beam experience slightly different frequencies. A similar effect is what causes the siren of an approaching ambulance to apparently change pitch as it passes you in the street. In their previous measurement in 2006, the ASACUSA team used just one laser beam, and the achievable accuracy was dominated by this effect. This time they used two beams moving in opposite directions, with the result that the jiggle for the two beams partly cancelled out, resulting in a four times better accuracy.

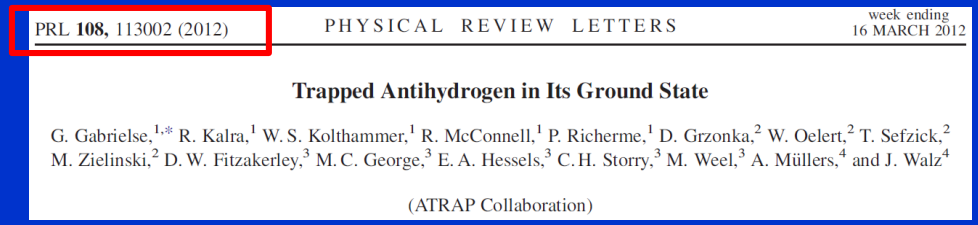

PRL **108,** 113002 (2012) PHYSICAL REVIEW LETTERS week ending 16 MARCH 2012

Trapped Antihydrogen in Its Ground State

G. Gabrielse,[1,*] R. Kalra,[1] W. S. Kolthammer,[1] R. McConnell,[1] P. Richerme,[1] D. Grzonka,[2] W. Oelert,[2] T. Sefzick,[2] M. Zielinski,[2] D. W. Fitzakerley,[3] M. C. George,[3] E. A. Hessels,[3] C. H. Storry,[3] M. Weel,[3] A. Müllers,[4] and J. Walz[4]

(ATRAP Collaboration)

ALPHA experiment shows antihydrogen charge is neutral

21 Jan 2016 – ALPHA shows the most accurate measurement yet of the electric charge of antihydrogen atoms in a new Nature paper

Updates related to ALPHA

The ALPHA experiment explores the secrets of antimatter

3 Aug 2017 – The ALPHA experiment at CERN's Antiproton Decelerator reports the first observation of the hyperfine structure of antihydrogen

ALPHA observes light spectrum of antimatter for first time

19 Dec 2016 – In a Nature paper, the ALPHA collaboration reports the first ever measurement on the optical spectrum of an antimatter

CERN's ALPHA experiment measures charge of antihydrogen

3 Jun 2014 – ALPHA reports a measurement of the electric charge of antihydrogen atoms, finding it to be compatible with zero to eight decimal places

ALPHA: Novel investigation of gravity and antimatter

30 Apr 2013 – The ALPHA collaboration has published a paper describing the first direct analysis of how antimatter is affected by gravity

Antimatter experiments present progress

15 Jan 2013 – At CERN today, the experiments at the Antiproton Decelerator presented updates on their work in 2012, and their hopes for 2013

The ALPHA experiment is a successor of an earlier antimatter experiment, ATHENA. Set up in late 2005 with similar overall research goals as its predecessor, ALPHA makes, captures and studies atoms of antihydrogen and compares these with hydrogen atoms.

Creating antihydrogen depends on bringing together the two component antiparticles, antiprotons and positrons, in a trapping device for charged particles. Since antihydrogen atoms have no electric charge, once they form they can't be confined in such a device. In the ATHENA experiment the antiatoms would drift naturally to the walls of the trap. Because these walls were made of ordinary matter, the contact caused the antiatoms to annihilate a few microseconds after they were created.

ALPHA is picking up from where ATHENA left off. ALPHA uses a different trapping method to hold the antihydrogen atoms, and will keep them for a longer period before they annihilate with ordinary atoms.

In June 2011, ALPHA reported that it had succeeded in trapping antimatter atoms for over 16 minutes: long enough to begin to study their properties in detail. This should give the physicists time to take measurements and to find more answers to the antimatter mystery.

Voir en français

2017

LETTER

OPEN

doi:10.1038/nature23446

Observation of the hyperfine spectrum of antihydrogen

M. Ahmadi[1], B. X. R. Alves[2], C. J. Baker[3], W. Bertsche[4,5], E. Butler[6], A. Capra[7], C. Carruth[8], C. L. Cesar[9], M. Charlton[3], S. Cohen[10], R. Collister[7], S. Eriksson[3], A. Evans[11], N. Evetts[12], J. Fajans[8], T. Friesen[2], M. C. Fujiwara[7], D. R. Gill[7], A. Gutierrez[12,13], J. S. Hangst[2], W. N. Hardy[12], M. E. Hayden[14], C. A. Isaac[3], A. Ishida[15], M. A. Johnson[4,5], S. A. Jones[3], S. Jonsell[16], L. Kurchaninov[7], N. Madsen[3], M. Mathers[17], D. Maxwell[3], J. T. K. McKenna[7], S. Menary[17], J. M. Michan[7,18], T. Momose[12], J. J. Munich[14], P. Nolan[1], K. Olchanski[7], A. Olin[7,19], P. Pusa[1], C. Ø. Rasmussen[2], F. Robicheaux[20], R. L. Sacramento[9], M. Sameed[3], E. Sarid[21], D. M. Silveira[9], S. Stracka[7,22], G. Stutter[2], C. So[11], T. D. Tharp[23], J. E. Thompson[17], R. I. Thompson[11], D. P. van der Werf[3,24] & J. S. Wurtele[8]

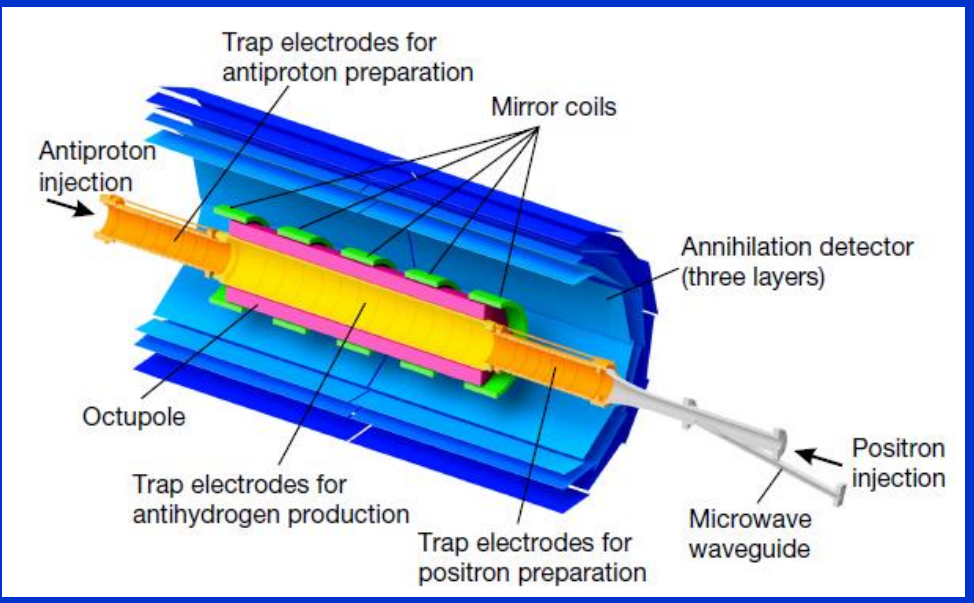

Figure 1 | The ALPHA-2 central apparatus. A cut-away schematic of the antihydrogen production and trapping region of ALPHA-2 is shown. For clarity, the vacuum wall and the cryostat for the superconducting magnets are not shown. Antiproton and positron plasmas are prepared on either side of the production region before being mixed to form antihydrogen at the centre of the minimum-*B* trap. All of the components shown are immersed in a uniform, 1-T, axial magnetic field, which is provided by an external solenoid (not illustrated).

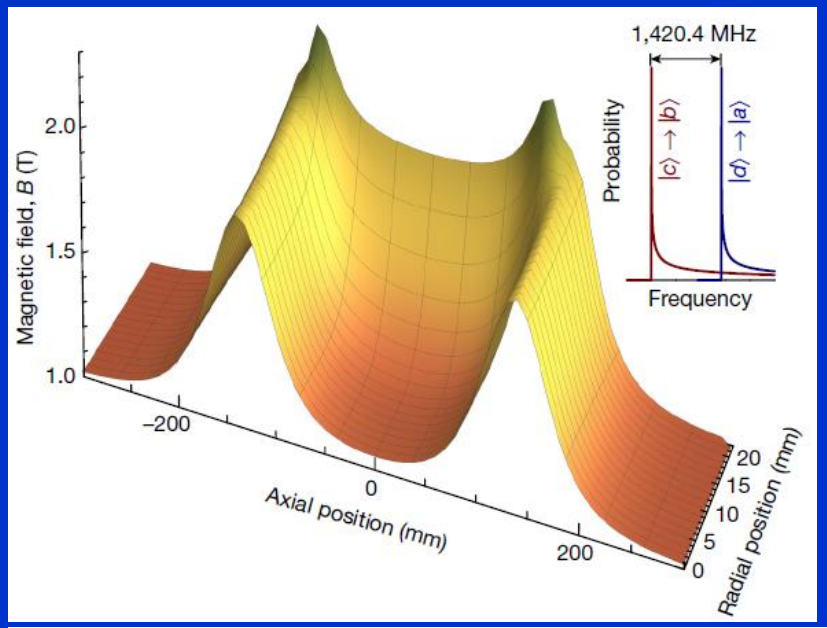

Figure 3 | Magnetic field strength. The scalar magnitude of the total magnetic field in the atom trap is plotted versus position. The radial position is measured from the symmetry axis of the trap, and the axial origin is the centre of the atom trap, defined by the outermost mirror coils. Inset, the probability of an atom being resonant at a given frequency, calculated for hydrogen; the two low-frequency onsets are separated by the ground-state splitting.

nature COMMUNICATIONS

ARTICLE

DOI: 10.1038/s41467-017-00760-9 OPEN

Antihydrogen accumulation for fundamental symmetry tests

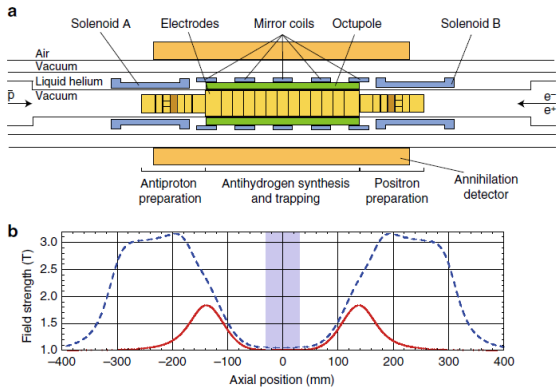

Fig. 1 The ALPHA-2 central apparatus. **a** ALPHA-2 geometry, drawn to scale except for the radial extent of the annihilation detector. The inner diameter of the Penning–Malmberg electrodes is 44.35 mm in the central region of the atom trap and 29.6 mm at either end. Antiprotons enter from the *left* in this view, while positrons and electrons are loaded from the *right*. **b** Magnetic field strength on axis with the atom trap energised (the external solenoid responsible for producing a uniform 1 T field is not shown). The *solid curve* (*red*) shows the flattened atom trap field used in ref. [5]. The *dashed curve* (*blue*), shows the on-axis field during stacking; the *left* and *right* solenoids **a**, **b** increase the field from 1 to 3 T for enhanced capture, cyclotron cooling and rotating wall efficiency of, as appropriate, positrons, electrons and antiprotons

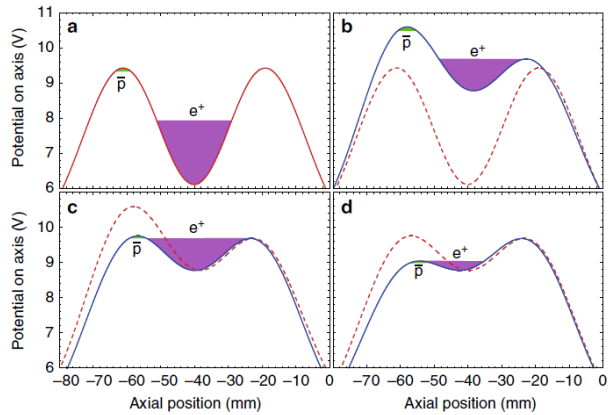

Fig. 2 Antihydrogen synthesis sequence. *Dashed* and *solid curves* represent electrostatic potentials before and after each step in the process. *Filled regions* indicate self-potentials and physical extents of antiproton and positron plasmas. **a** Potential before evaporative cooling. Positron well depth 3.31 V. **b** Evaporative cooling, during which energetic positrons escape to the right (duration 600 ms). Final positron well depth 0.91 V. **c** Potential realignment in preparation for mixing (duration 10 ms). Final positron well depth 0.91 V. **d** Potential merge mixing (duration 1 s). Positrons escape to the left during mixing, resulting in further evaporative cooling. Final positron well depth 0.27 V. Remaining positrons are ejected to the right for a temperature measurement; remaining antiprotons are ejected to the left

Table 1 Figures of merit characterising antihydrogen formation and trapping efficiencies

$\bar{p}$ injected (×10⁴)	$\bar{H}$ formed (×10⁴)	T_{e^+} before (K)	T_{e^+} after (K)	Number of trials	$\bar{H}$ trapped & detected	$\bar{H}$ trapping efficiency (× 10⁻⁴)
AR injection mixing[a]						
1.31 ± 0.01	0.53 ± 0.01	27 ± 3	51 ± 1	54	0.62 ± 0.11	1.6 ± 0.3
3.1 ± 0.1	0.87 ± 0.01	27 ± 3	60 ± 1	27	0.59 ± 0.15	0.9 ± 0.2
Potential merge mixing[b]						
5.5 ± 0.1	2.4 ± 0.1	18 ± 2	16 ± 1	16	8.7 ± 0.7	4.7 ± 0.4
9.0 ± 0.3	3.1 ± 0.1	18 ± 2	17 ± 1	26	10.5 ± 0.6	4.7 ± 0.3

Antiprotons were evaporatively cooled to ~40 K in all cases. [a]AR injection mixing. The positron plasma comprised 2.3×10^6 positrons at a density of 1.3×10^8 cm^{-3} and a radius of 0.55 mm. [b]1 s potential merge mixing. The positron plasma comprised 1.6×10^5 positrons at a density of 6.5×10^7 cm^{-3} and a radius of 0.66 mm. The trapping efficiency is the number of trapped antihydrogen divided by the number formed (annihilation detector efficiencies included). The positron densities were set by tuning the evaporative cooling process to achieve maximum trapping efficiency. Uncertainties are statistical and assume the parent distributions are Poissonian

The observation of hyperfine structure in atomic hydrogen by Rabi and co-workers[1–3] and the measurement[4] of the zero-field ground-state splitting at the level of seven parts in 10^{13} are important achievements of mid-twentieth-century physics. The work that led to these achievements also provided the first evidence for the anomalous magnetic moment of the electron[5–8], inspired Schwinger's relativistic theory of quantum electrodynamics[9,10] and gave rise to the hydrogen maser[11], which is a critical component of modern navigation, geo-positioning and very-long-baseline interferometry systems. Research at the Antiproton Decelerator at CERN by the ALPHA collaboration extends these enquiries into the antimatter sector. Recently, tools have been developed that enable studies of the hyperfine structure of antihydrogen[12]—the antimatter counterpart of hydrogen. The goal of such studies is to search for any differences that might exist between this archetypal pair of atoms, and thereby to test the fundamental principles on which quantum field theory is constructed. Magnetic trapping of antihydrogen atoms[13,14] provides a means of studying them by combining electromagnetic interaction with detection techniques that are unique to antimatter[12,15]. Here we report the results of a microwave spectroscopy experiment in which we probe the response of antihydrogen over a controlled range of frequencies. The data reveal clear and distinct signatures of two allowed transitions, from which we obtain a direct, magnetic-field-independent measurement of the hyperfine splitting. From a set of trials involving 194 detected atoms, we determine a splitting of $1{,}420.4 \pm 0.5$ megahertz, consistent with expectations for atomic hydrogen at the level of four parts in 10^4. This observation of the detailed behaviour of a quantum transition in an atom of antihydrogen exemplifies tests of fundamental symmetries such as charge–parity–time in antimatter, and the techniques developed here will enable more-precise such tests.

In an earlier experiment[12] using the original ALPHA apparatus[16], we demonstrated microwave-induced spin flips in trapped antihydrogen. The current work was carried out using the second-generation ALPHA-2 device (Fig. 1), operating at the CERN Antiproton Decelerator[17]. Unlike their matter counterparts, antihydrogen atoms must be synthesized[18] by merging cold plasmas of antiprotons and positrons in specially configured Penning–Malmberg traps. In the ALPHA-2 device, we typically mix 90,000 antiprotons, slowed and captured from the Antiproton Decelerator, with 1.6 million positrons from a Surko-type accumulator[19] to produce about 25,000 antihydrogen atoms. These numbers are monitored in daily baseline measurements that involve ejecting particles onto a multichannel plate detector.

Of the produced antihydrogen atoms, only a few will have low enough kinetic energies (0.54 K in temperature units) to be trapped in our superconducting, multipolar, magnetic-minimum trap. The current state-of-the-art is that about 20 atoms can be trapped from a single mixing sequence, and we have accumulated up to 74 atoms by repetitive mixing (M.A. *et al.*, submitted). A single mixing and capture sequence takes approximately 4 min, the bulk of which is used for preparation of plasmas of appropriate temperature, size and density (M.A. *et al.*, submitted). The actual mixing process takes less than 1 s. The trapped antimatter atoms can survive for at least 1,000 s in the cryo-pumped ultrahigh vacuum of ALPHA-2.

Referring to Fig. 1, the antiproton and positron plasmas are merged in the central Penning trap (yellow electrodes) to produce antihydrogen. An external solenoid magnet provides a uniform 1-T field for the Penning trap. The production region is near the centre of the magnetic-minimum trap, which comprises an octupole coil for transverse confinement of neutral anti-atoms and five short solenoids ('mirror coils') that can shape the axial trapping well. The trapping volume is cylindrical, with a diameter of 44.35 mm and length of 280 mm. For the current experiment, only the outer two mirror coils are used to create the axial well.

Antihydrogen atoms that leave the trap and annihilate on the electrodes of the Penning trap are registered by the ALPHA-2 annihilation detector[20]. This three-layer silicon vertex detector that

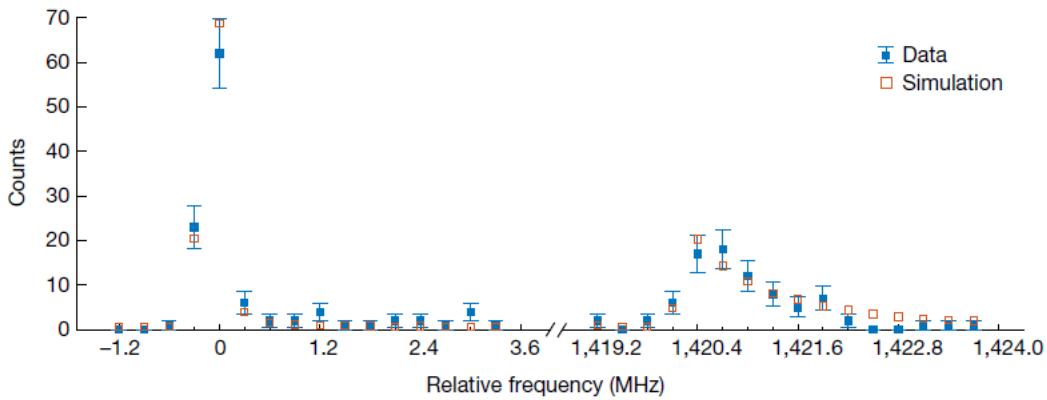

Figure 4 | Data and simulation. The number of detected antihydrogen annihilation events (filled blue squares), summed (see the text for details) over 22 trials, is plotted as a function of frequency. Note the discontinuous abscissa. The error bars represent counting statistics only. The expectations from the simulation for hydrogen in the trap are also shown (open red squares). The simulation results are scaled to match the total number (194) of observed events and are aligned to match the onset of the lower transition. The simulation includes the effect of measured fluctuations in the currents in the trapping magnets.

ALPHA trap

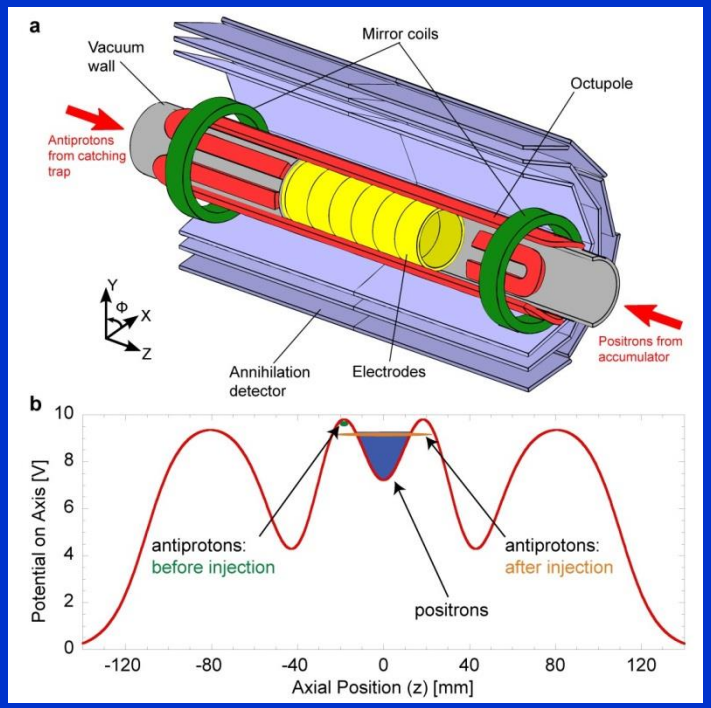

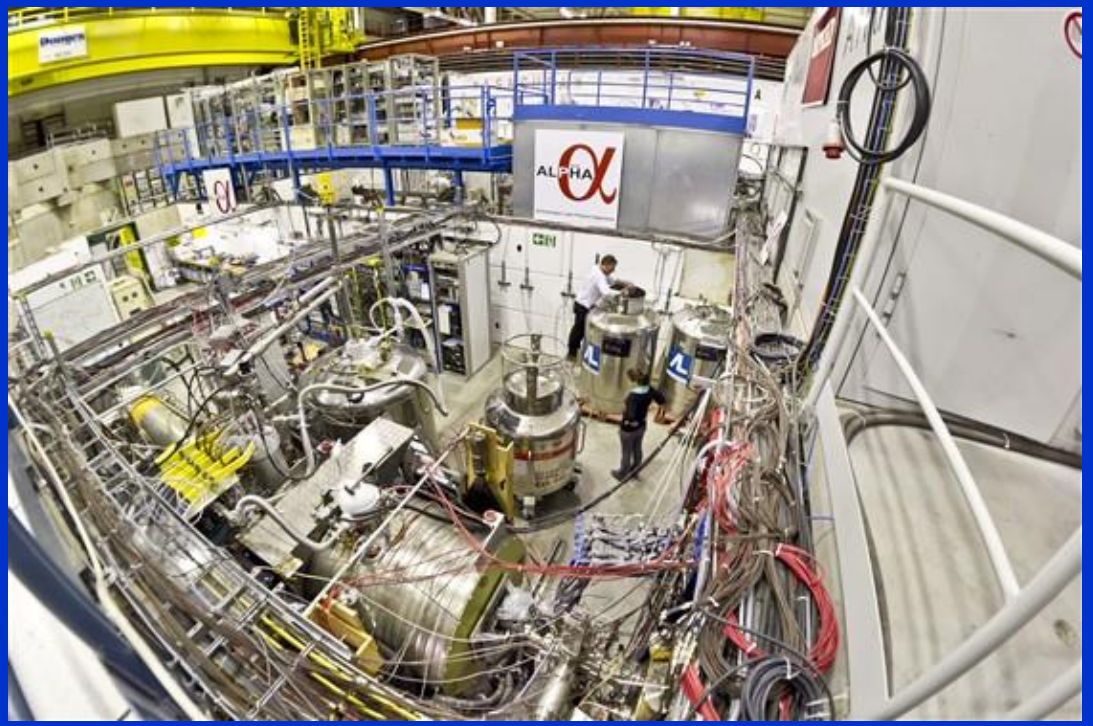

a. An illustration of the inner mixing trap electrodes surrounded by the octopole and mirror coil magnets as well as the Silicon detector.
b. b. A plot of the on axis electric potential in the mixing trap region.
Figure from: Andresen et al., "Trapped Antihydrogen" *Na*ture, 2010

Resonant quantum transitions in trapped antihydrogen atoms

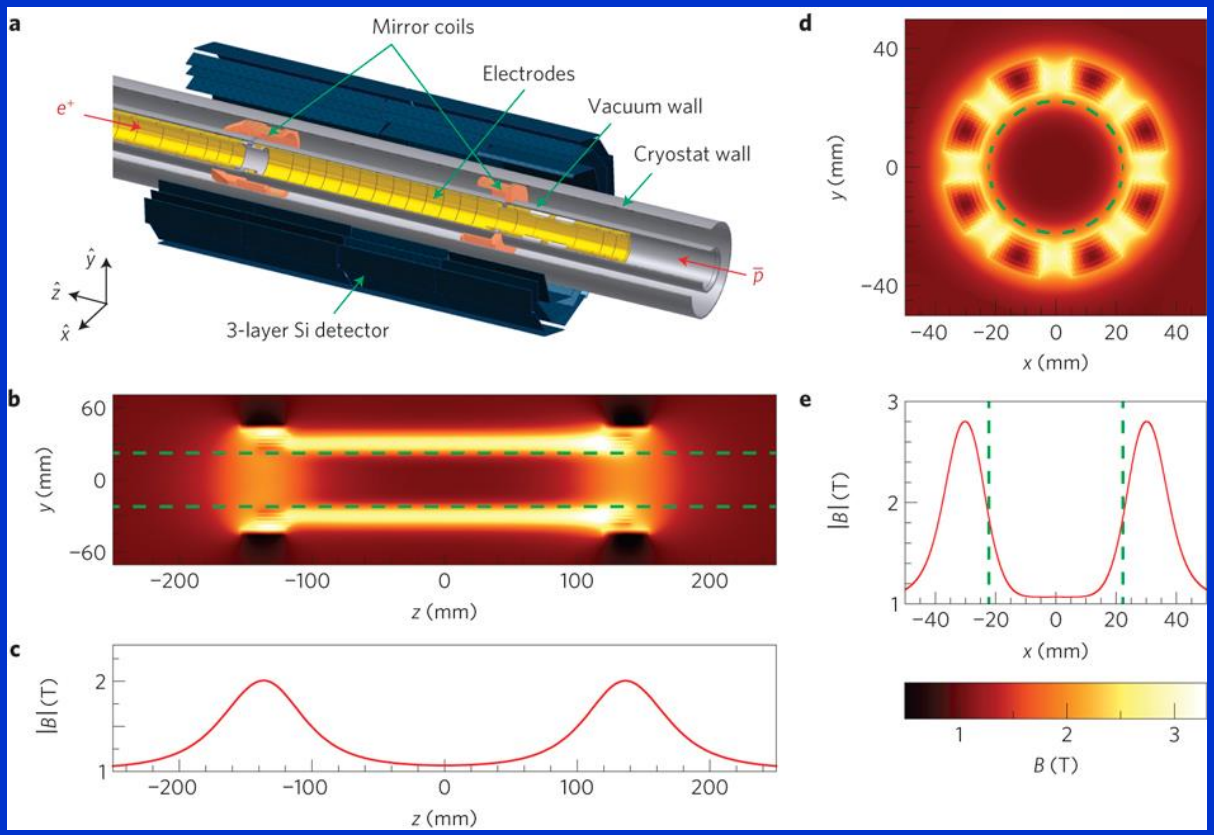

Figure 1: The ALPHA antihydrogen trap and its magnetic-field configuration.

a, A schematic view of the ALPHA trap. Radial and axial confinement of antihydrogen atoms is provided by an octupole magnet (not shown) and mirror magnets, respectively. Penning trap electrodes are held at ~9 K, and have an inner diameter of 44.5 mm. A three-layer silicon vertex detector surrounds the magnets and the cryostat. A 1 T base field is provided by an external solenoid (not shown). An antiproton beam is introduced from the right, whereas positrons from an accumulator are brought in from the left.
b, The magnetic-field strength in the *y*–*z* plane (*z* is along the trap axis, with *z*=0 at the centre of the magnetic trap). Green dashed lines in this and other figures depict the locations of the inner walls of the electrodes.
c, The axial field profile, with an effective trap length of ~270 mm.
d, The field strength in the *x*–*y* plane.
e, The field-strength profile along the *x* axis.

THE ALPHA COLLABORATION

Aarhus University, Denmark

University of British Columbia, Canada

University of California Berkeley, USA

University of Calgary, Canada

Imperial College London

University of Liverpool, UK

University of Manchester, UK

NRCN - Nuclear Res. Center Negev, Israel

Purdue University, West Lafayette, USA

Federal University of Rio de Janeiro, Brazil

Stockholm University, Sweden

Simon Fraser University, Canada `

TRIUMF, Canada

University of Wales Swansea, UK

Cockcroft Institute, UK

York University, Canada

Three-body recombination FP II 1 2018

Recombination of antiprotons with positrons at low temperatures

B Zygelman[1]

$$A^+ + e + e \rightarrow (A^+ + e)^n + e(\varepsilon) \rightarrow A + e$$

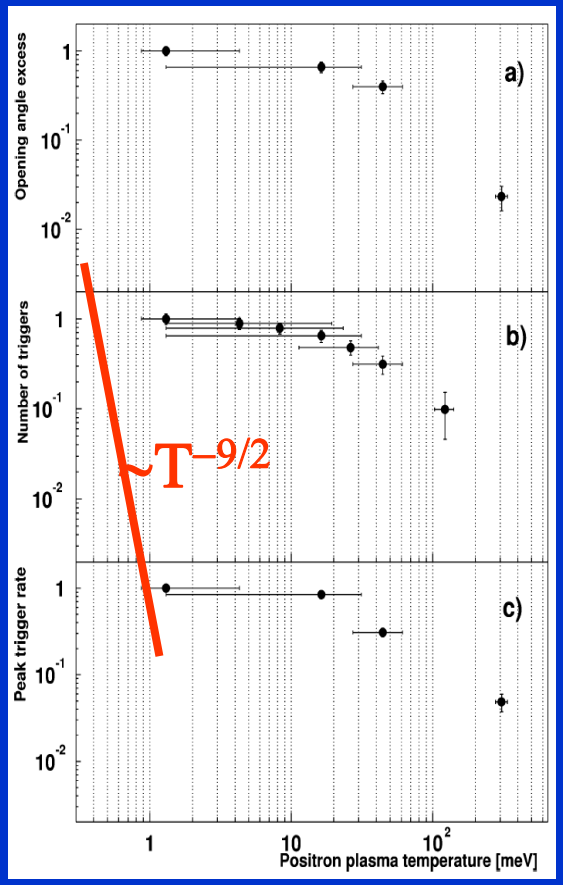

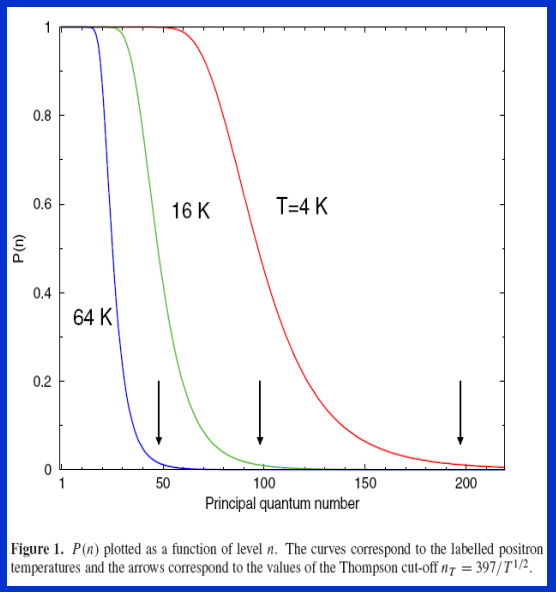

Figure 1. $P(n)$ plotted as a function of level n. The curves correspond to the labelled positron temperatures and the arrows correspond to the values of the Thompson cut-off $n_T = 397/T^{1/2}$.

Based on the results of our calculations, we suggest that the ground state recombination coefficient is more accurately described by the relation

$$\alpha = \frac{\alpha_0}{1 + \tilde{\tau} n_{\tilde{e}} \alpha_0} \qquad (17)$$

which reduces to the standard form $\alpha = \alpha_0 \sim n_{\tilde{e}}/T^{9/2}$ when $\tilde{\tau} \ll 1/n_{\tilde{e}}\alpha_0$. Our conclusion is in harmony with an observation of Flannery and Vrinceanu [15], that the total recombination rate is controlled by the limiting rate of the recombination cascade.

Temperature dependence of anti-H production using different variables.


Quo vadis ?

$Ar^+ + e^- + e^-$

$H^+ + e^- + e^-$

Anti hydrogen formation

Colisional Radiative Recombination -CRR

$$\frac{dn_e}{dt} = -K_{CRR}\ [Ar^+]\, n_e^2 - \frac{n_e}{\tau_D} = -K_{CRR}\ \ n_e^3 - \frac{n_e}{\tau_D}$$

$$\alpha_{CRR} = K_{CRR}\, n_e$$

PRL 98, 133201 (2007) PHYSICAL REVIEW LETTERS week ending 30 MARCH 2007

$H^+ + e^- + e^- \rightarrow H + e^-$

Three-Body Recombination of Atomic Ions with Slow Electrons **2007**

S. X. Hu
Laboratory for Laser Energetics, University of Rochester, 250 East River Road, Rochester, New York 14623, USA

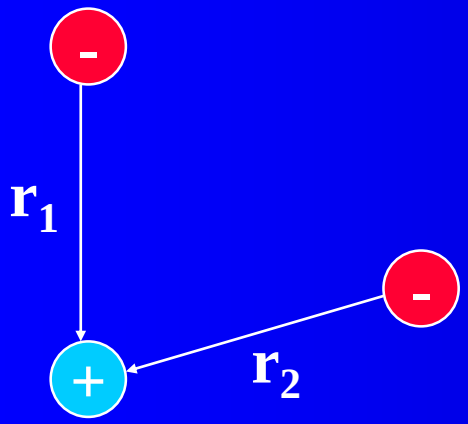

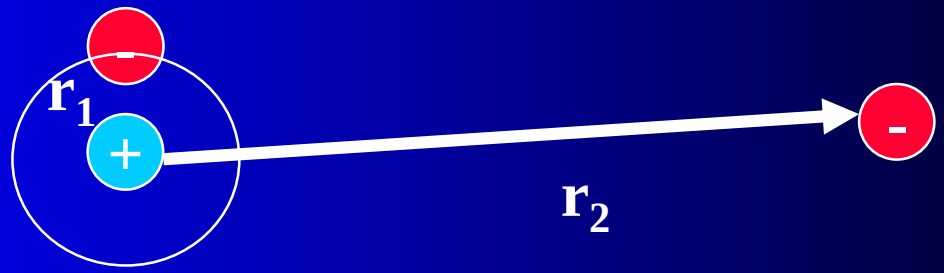

We consider the simplest TBR in the case of hydrogen formation, in which two free electrons interact with a proton. To investigate the three-body interaction dynamics, we numerically solve the six-dimensional (6D) time-dependent Schrödinger equation, which has the following form (atomic units are used throughout):

$$i\frac{\partial}{\partial t}\Phi(\mathbf{r}_1, \mathbf{r}_2, t) = \left[-\frac{1}{2}(\Delta_{\mathbf{r}_1} + \Delta_{\mathbf{r}_2}) - \frac{1}{r_1} - \frac{1}{r_2} + \frac{1}{|\mathbf{r}_1 - \mathbf{r}_2|}\right]\Phi(\mathbf{r}_1, \mathbf{r}_2, t), \quad (1)$$

where $\mathbf{r}_1$ and $\mathbf{r}_2$ are the position vectors of each electron, with respect to the proton. We obtain a more tractable with respect to the proton. We obtain a more tractable solution by using the close-coupling recipe [12]: expanding the 6D wave function $\Phi(\mathbf{r}_1, \mathbf{r}_2|t)$ in terms of bipolar spherical harmonics $Y^{LS}_{l_1 l_2}(\Omega_1, \Omega_2)$, $\Phi(\mathbf{r}_1, \mathbf{r}_2|t) = \sum_{LS}\sum_{l_1 l_2}[\Psi^{(LS)}_{l_1 l_2}(r_1, r_2|t)/r_1 r_2]Y^{LS}_{l_1 l_2}(\Omega_1, \Omega_2)$, for a specific symmetry (LS). We can also expand the Coulomb repulsion term $1/|\mathbf{r}_1 - \mathbf{r}_2|$ in terms of spherical harmonics. Substituting these expansions into the above Schrödinger Eq. (1) and integrating over the angles Ω_1 and Ω_2 yields a set of coupled partial differential equations with only two radial variables r_1 and r_2 left:

$$i\frac{\partial}{\partial t}\Psi_j(r_1, r_2|t) = [\hat{T}_1 + \hat{T}_2 + \hat{V}_c]\Psi_j(r_1, r_2|t) + \sum_k \hat{V}^I_{j,k}(r_1, r_2|t)\Psi_k(r_1, r_2|t), \quad (2)$$

where the partial-wave index j runs from 1 to the total number N of partial waves used for expansion. In Eq. (2),

$H^+ + e^- + e^- \rightarrow H + e^-$

$$i\frac{\partial}{\partial t}\Psi_j(r_1, r_2|t) = [\hat{T}_1 + \hat{T}_2 + \hat{V}_c]\Psi_j(r_1, r_2|t) + \sum_k \hat{V}^I_{j,k}(r_1, r_2|t)\Psi_k(r_1, r_2|t), \quad (2)$$

$$P_{nl}(E_2) = 2\sum_{LS}\sum_{l_2}\left|\int dr_1 \int dr_2 \phi^*_{nl}(r_1)\phi^*_{k_2 l_2}(r_2)\Psi^{(LS)}_{ll_2}(r_1, r_2, t = t_f)\right|^2,$$

K_E=0.1 eV

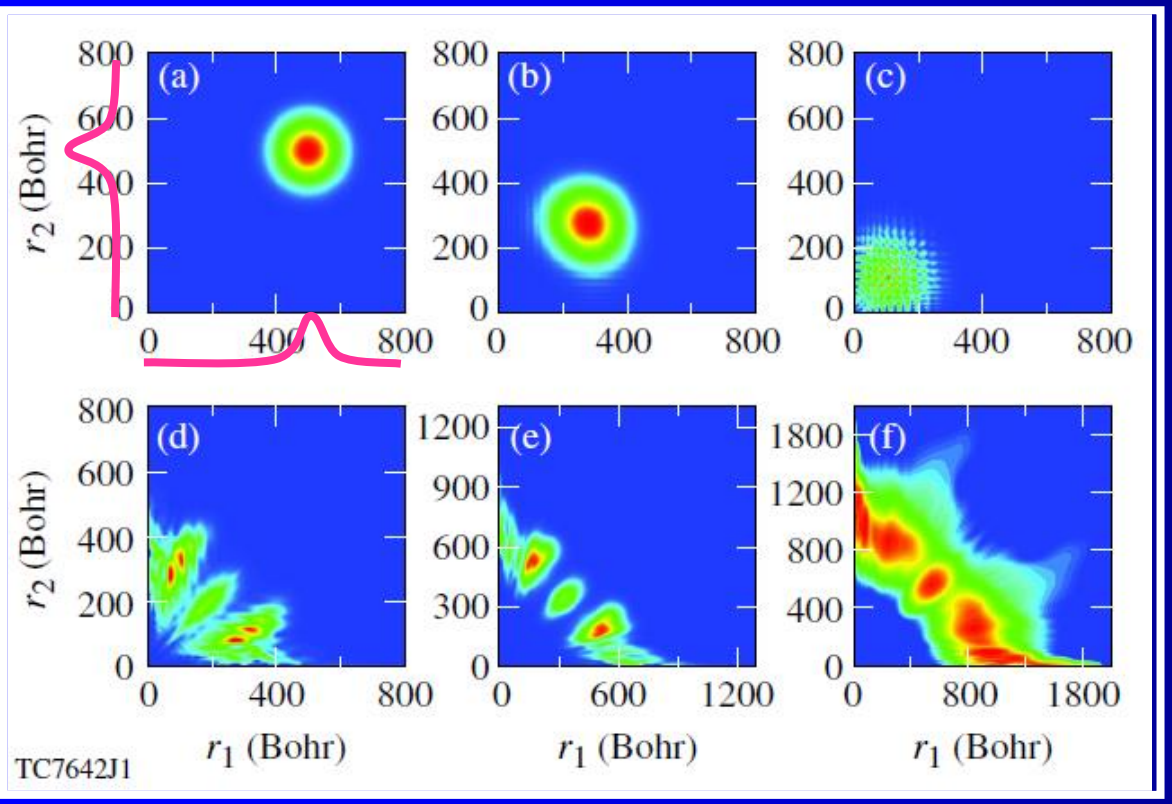

FIG. 1 (color online). Snapshots of electron probability distribution on the plane spanned by the radial coordinates r_1 and r_2 for different times: (a) $t = 0.0$ fs, (b) $t = 60$ fs, (c) $t = 100$ fs, (d) $t = 150$ fs, (e) $t = 194$ fs, and (f) (in log scale) $t = 260$ fs.

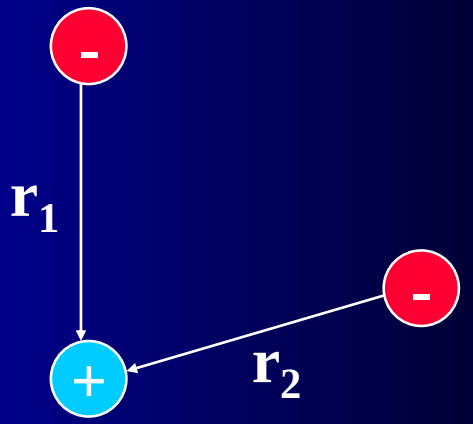

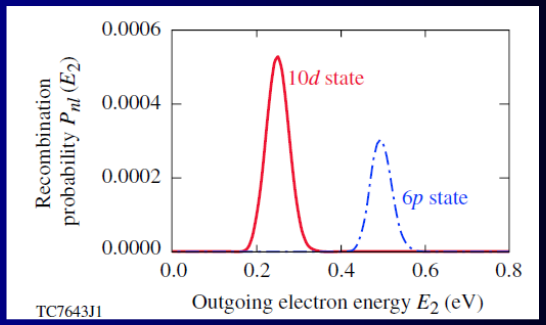

Thus, for the case of $K_E = 0.1$ eV considered in Figs. 1 and 2, the total system energy is about $E_{tot} \sim 0.12$ eV instead of $2K_E$. Hence, when one electron recombines to the 10d state ($|E_{10d}| \approx 0.136$ eV) of the H atom, the outgoing electron takes an initial total energy of 0.12 eV plus $|E_{10d}|$, thereby $P_{10d}(E_2)$ peaks at $E_2 \sim 0.256$ eV, as shown by the (red) solid line of Fig. 2. Similar energy conservation is also well satisfied for the recombination to the 6p state, as is illustrated by the (blue) dash-dotted line in Fig. 2. Our quantum calculations unambiguously reveal the essential feature of a TBR process.

$H^+ + e^- + e^- \rightarrow H + e^-$

$K_E = 0.1$ eV

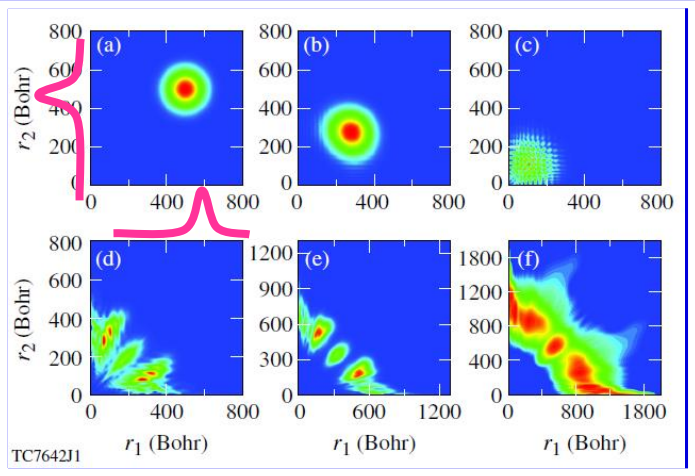

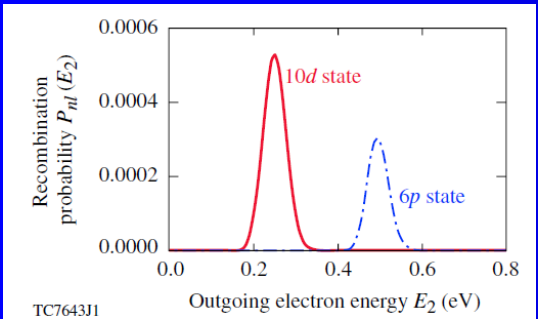

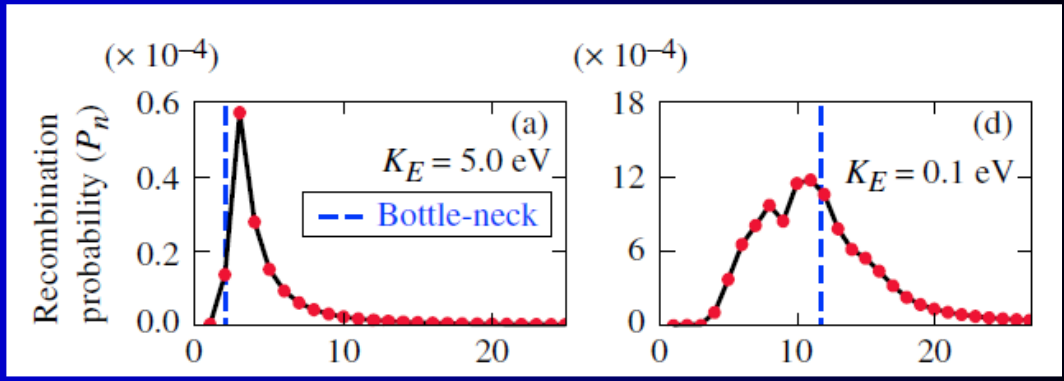

FIG. 3 (color online). The recombination probability P_n as a function of the energy level n, for different electron kinetic energies K_E marked in each panel.

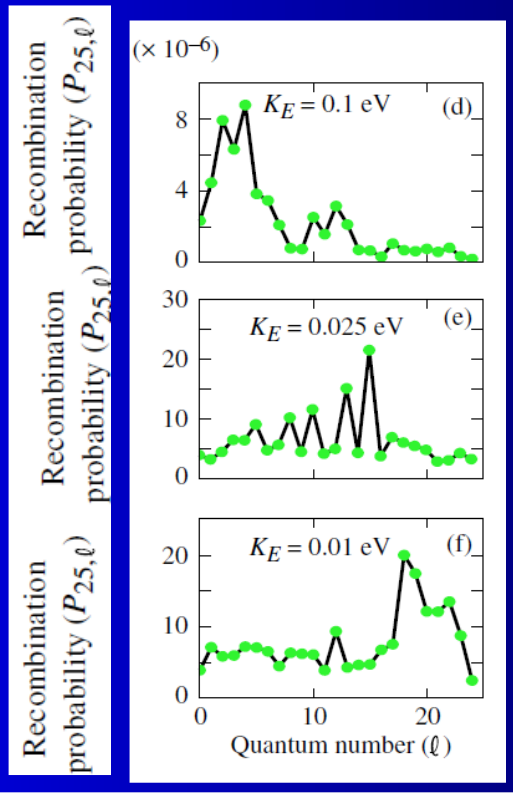

FIG. 4 (color online). The recombination probability $P_{n=25,l}$ as a function of the angular-momentum quantum number l, for different electron kinetic energies K_E marked in each panel.

$Ar^+ + e^- + e^-$

$H^+ + e^- + e^-$

Anti hydrogen formation

$$\frac{dn_e}{dt} = -K_{CRR}\,[Ar^+]n_e^2 - \frac{n_e}{\tau_D} = -K_{CRR}\,n_e^3 - \frac{n_e}{\tau_D}$$

$$\alpha_{CRR} = 3.8\times10^{-9}T_e^{-4.5}n_e + 1.55\times10^{-10}T_e^{-0.63} + 6\times10^{-9}T_e^{-2.18}n_e^{0.37}\,\mathrm{cm^3 s^{-1}}$$

$$K_{CRR} = 3.8\times10^{-9}T_e^{-4.5}\,\mathrm{cm^6 s^{-1}}$$

$$\alpha_{CRR} = K_{CRR}\,n_e$$

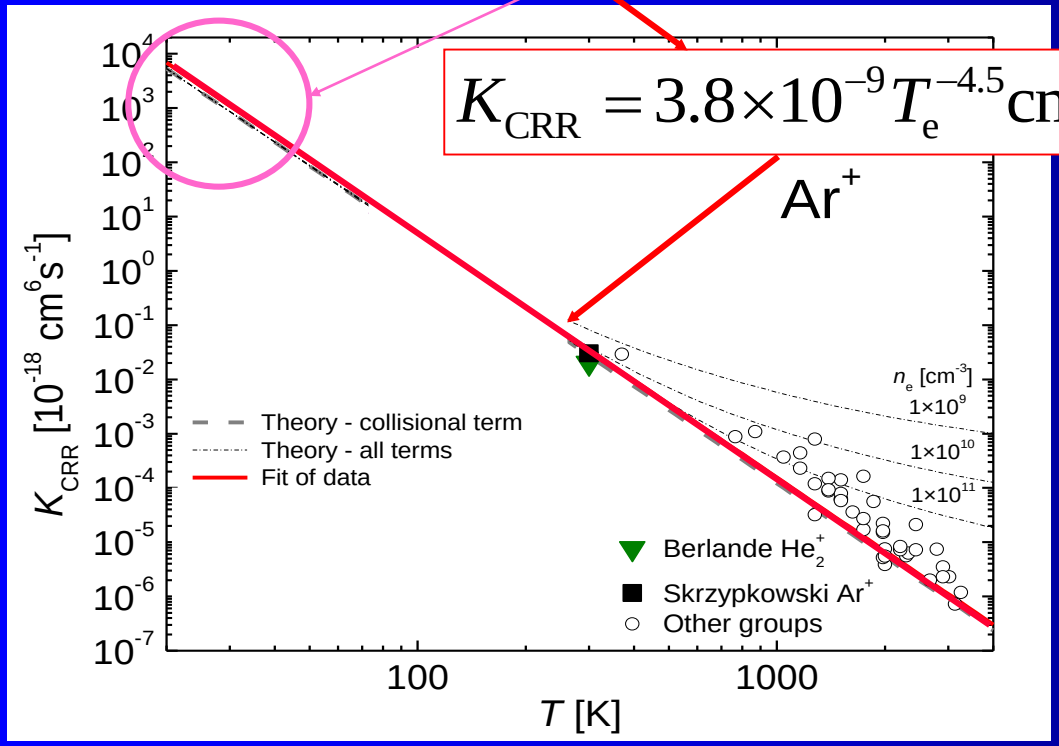

REALITA všedných dní

FP II 1- 2018

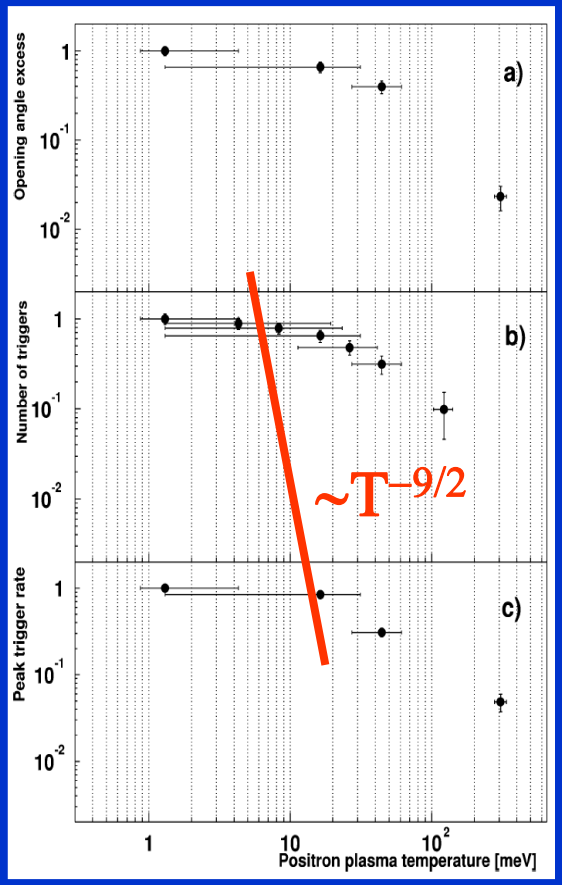

$$Ar^+ + e + e \rightarrow Ar + e$$

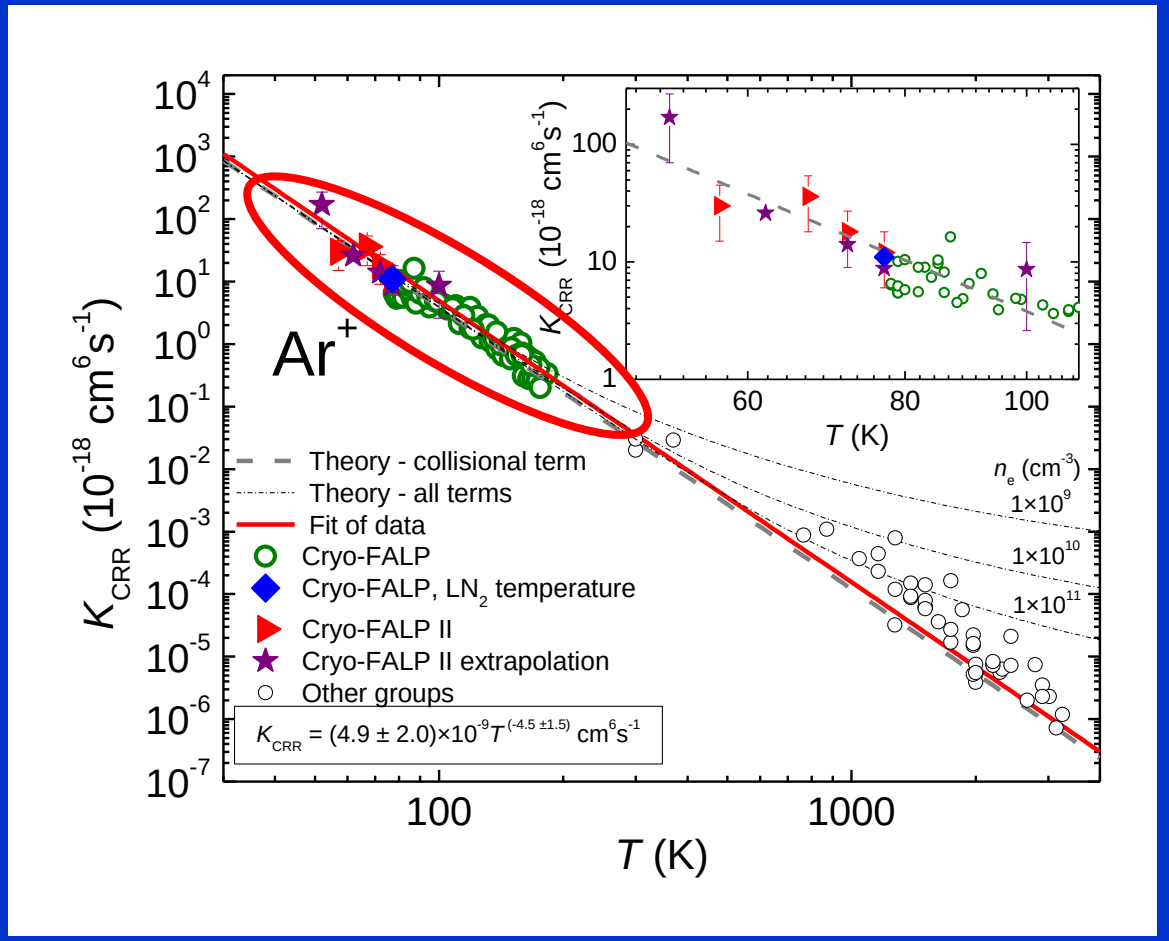

$$Ar^+ + e + e \rightarrow Ar + e$$

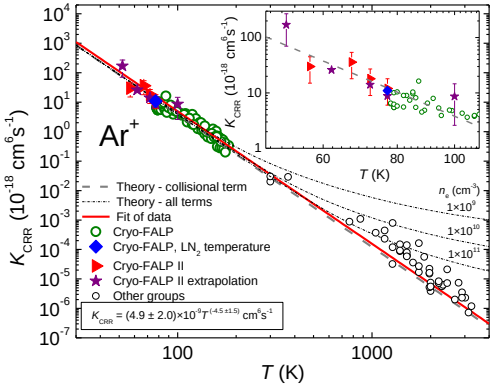

$$Ar^+ + e + He \rightarrow Ar + He$$

$$NO^+ + e + He \rightarrow N + O + He$$

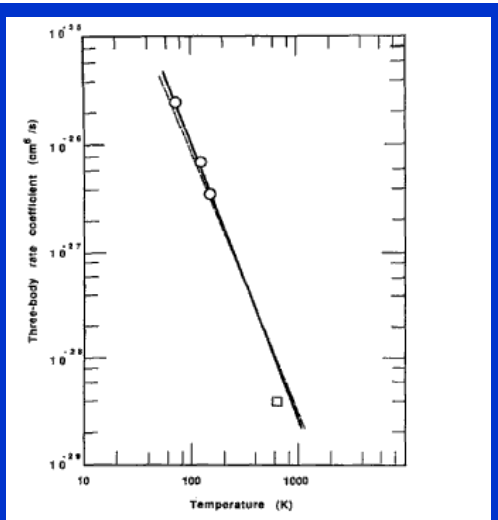

FIG. 4. The log–log graph of three-body recombination coefficients (slopes of the straight lines in Fig. 2) as a function of gas temperature. Circles— present data; square—the data point of Gousset *et al.* (Ref. 10); solid line—straight-line fit to present data; dashed line—scaled theory of Bates and Khare.

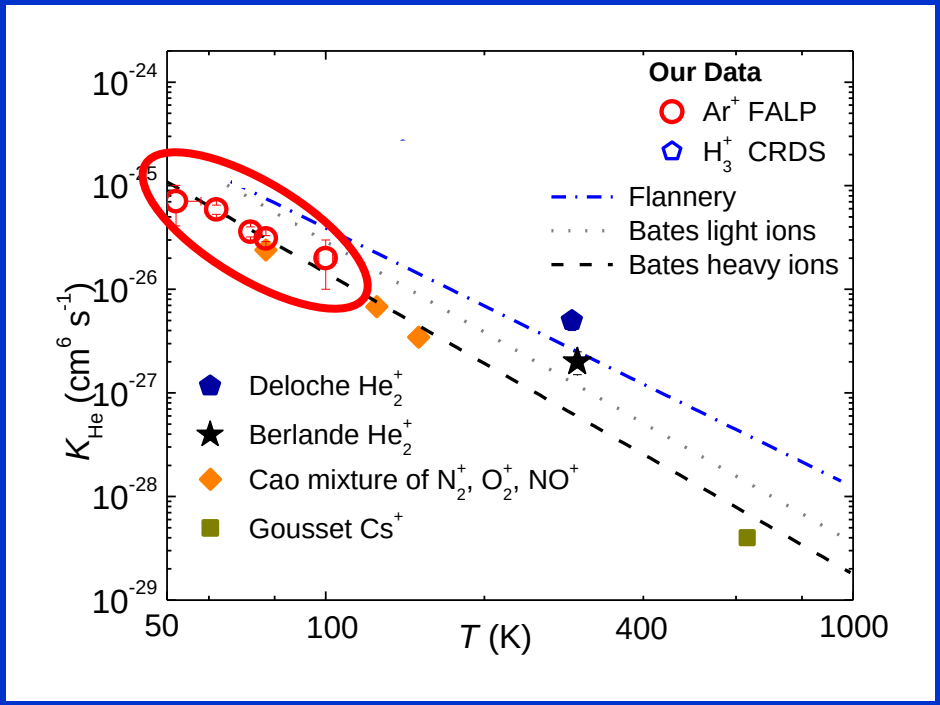

$Ar^+ + e^- + e^-$

$$\frac{dn_e}{dt} = -K_{CRR}\,[Ar^+]n_e^2 - \frac{n_e}{\tau_D} = -K_{CRR}\,n_e^3 - \frac{n_e}{\tau_D}$$

$$\alpha_{CRR} = 3.8\times10^{-9}T_e^{-4.5}n_e + 1.55\times10^{-10}T_e^{-0.63} + 6\times10^{-9}T_e^{-2.18}n_e^{0.37}\,\mathrm{cm^3s^{-1}}$$

$$K_{CRR} = 3.8\times10^{-9}T_e^{-4.5}\,\mathrm{cm^6s^{-1}}$$

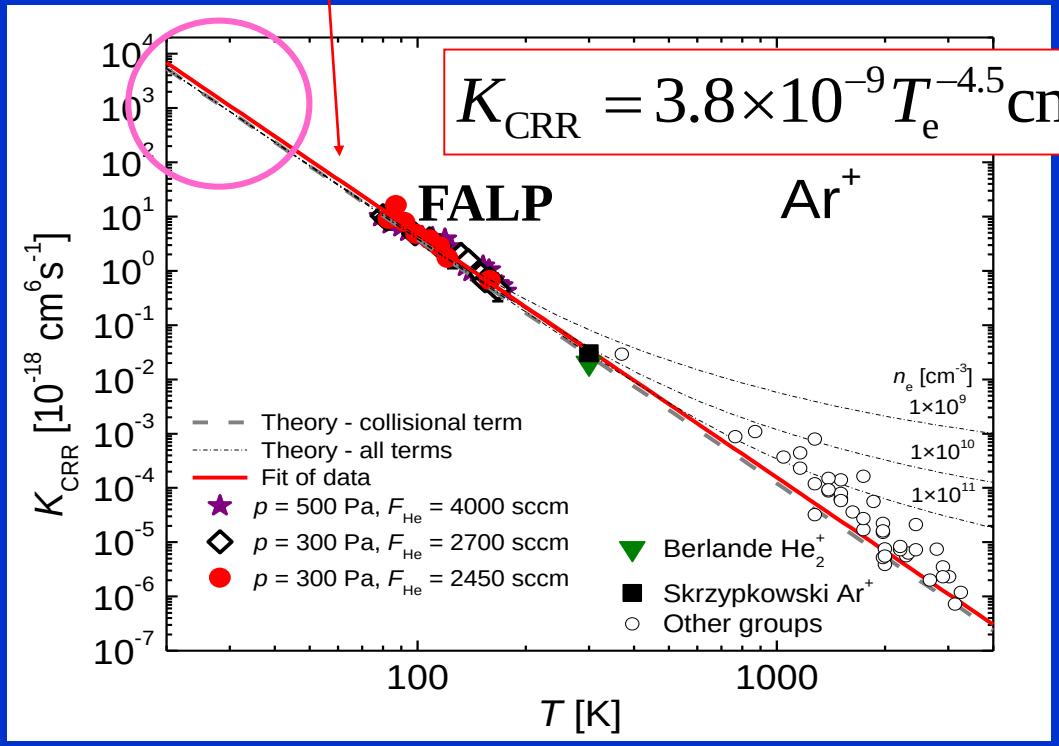

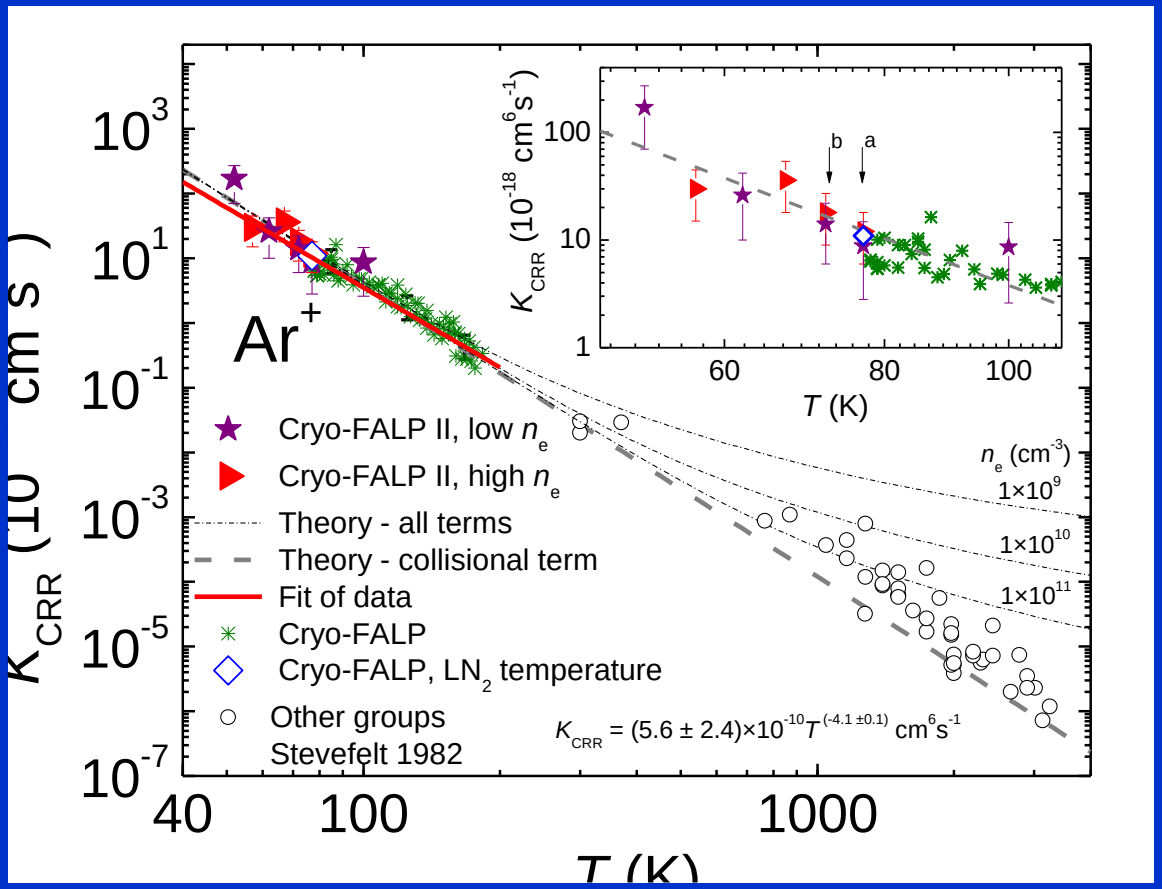
K_{CRR} (10^{-18} cm^{6}s^{-1})
10^3
10^1
10^{-1}
10^{-3}
10^{-5}
10^{-7}
Ar$^+$
Cryo-FALP II, low n_e
Cryo-FALP II, high n_e
Theory - all terms
Theory - collisional term
Fit of data
Cryo-FALP
Cryo-FALP, LN$_2$ temperature
Other groups
Stevefelt 1982
K_{CRR} = (5.6 ± 2.4)×10^{-10} $T^{(-4.1 \pm 0.1)}$ cm^{6}s^{-1}
n_e (cm^{-3})
1×10^9
1×10^{10}
1×10^{11}
40
100
1000
T (K)
K_{CRR} (10^{-18} cm^{6}s^{-1})
100
10
1
b
a
60
80
100
T (K)

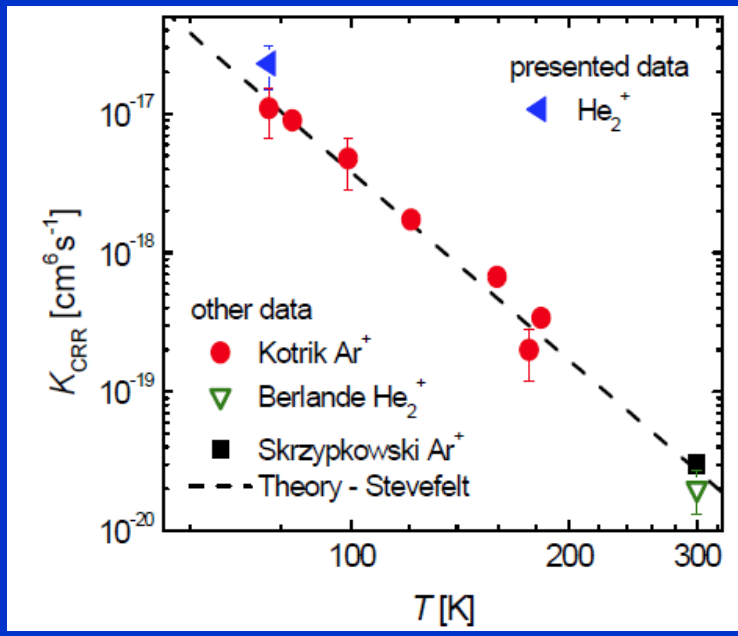
K_{CRR} [cm^{6}s^{-1}]
10^{-17}
10^{-18}
10^{-19}
10^{-20}
presented data
He$_2^+$
other data
Kotrik Ar$^+$
Berlande He$_2^+$
Skrzypkowski Ar$^+$
Theory - Stevefelt
100
200
300
T [K]

REALITA všedných dní

FP II 1- 2018

$$Ar^+ + e + e \rightarrow Ar + e$$

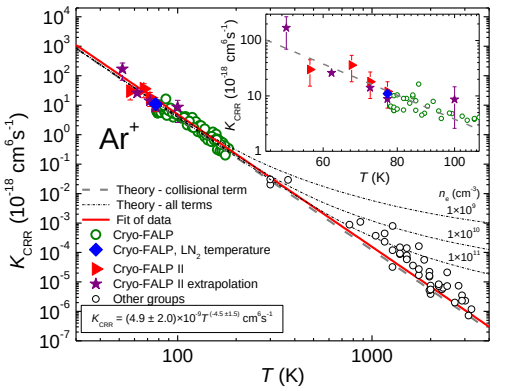

$$H_3^+ + e + He \rightarrow H + H + H + He$$

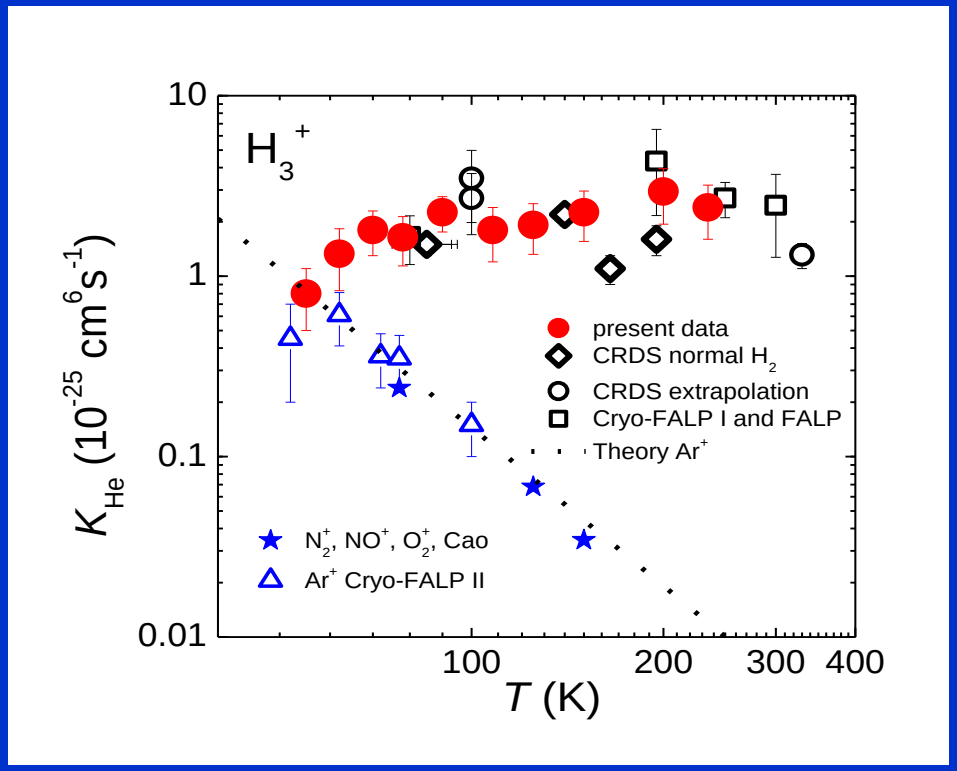

$$Ar^+ + e + He \rightarrow Ar + He$$

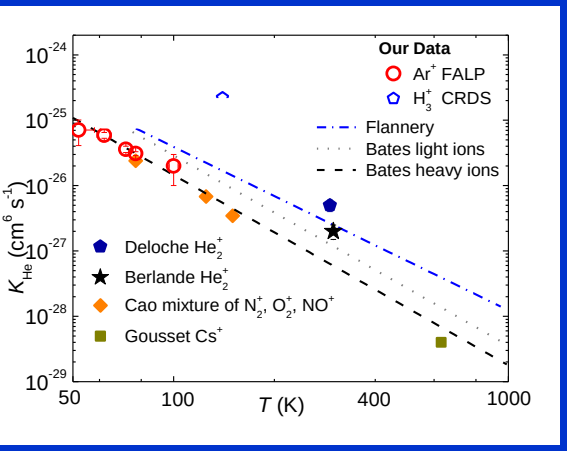

REALITA všedných dní

$$Ar^+ + e + e \rightarrow Ar + e$$

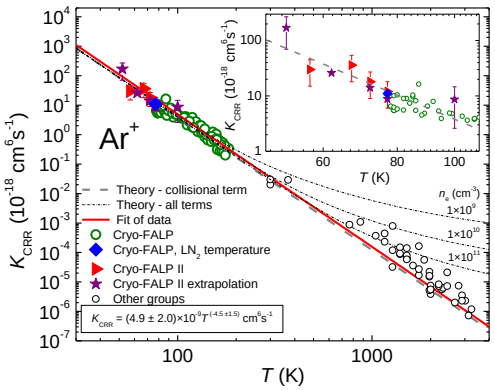

$$D_3^+ + e \rightarrow D + D + D, D + D_2$$

$$D_3^+ + e + He \rightarrow D + D + D + He$$

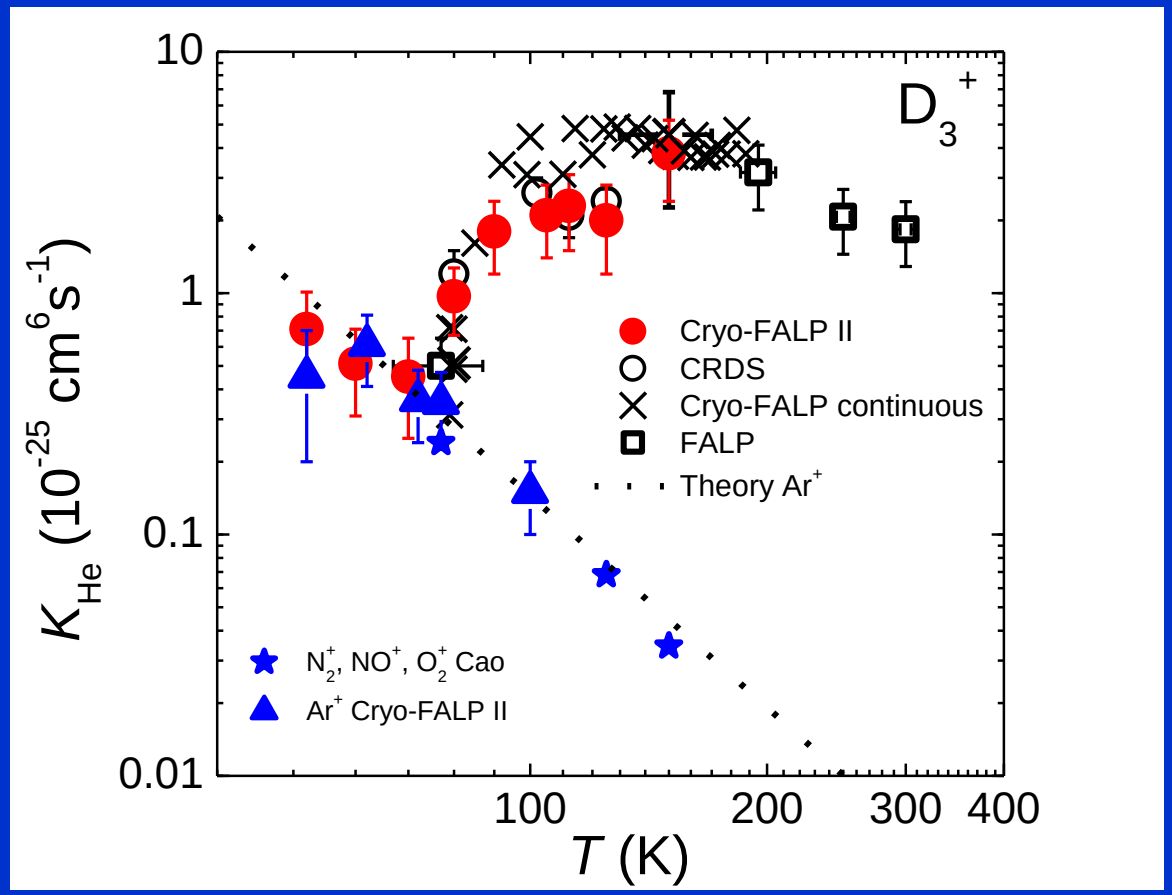

$$Ar^+ + e + He \rightarrow Ar + He$$

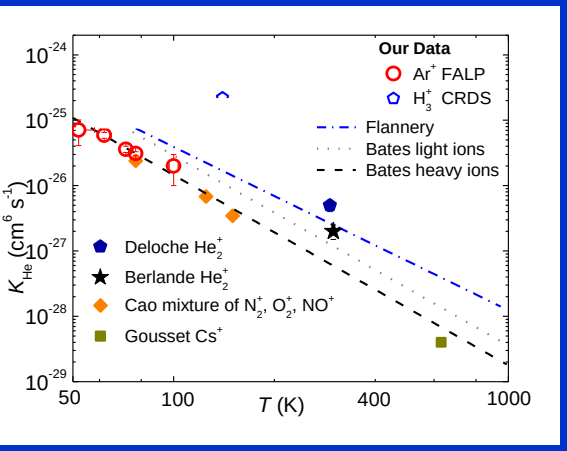

REALITA všedných dní

$$Ar^+ + e + e \rightarrow Ar + e$$

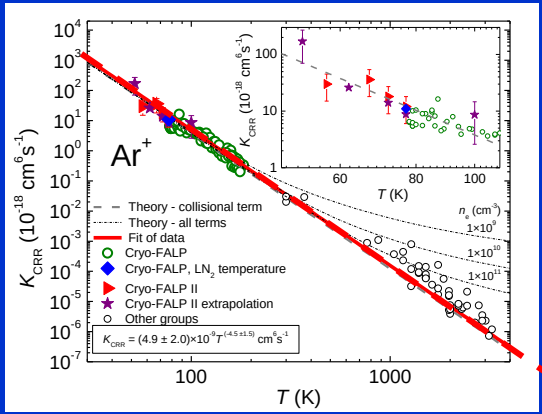

$\sim T^{-4.5}$

$$Ar^+ + e + He \rightarrow Ar + He$$

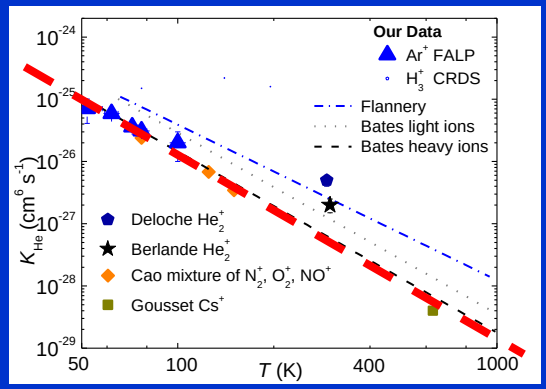

$\sim T^{-2.5}$

FP II 1- 2018

$$H_3^+ + e + He \rightarrow H + H + H + He$$

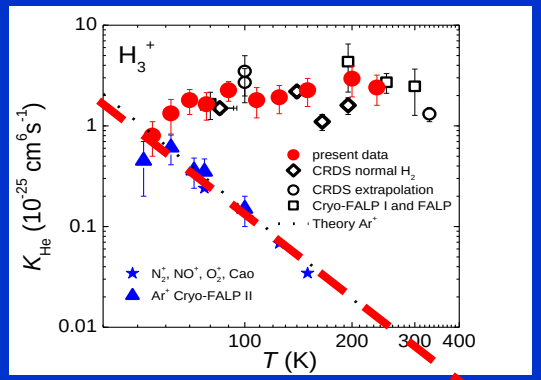

$$D_3^+ + e + He \rightarrow D + D + D + He$$

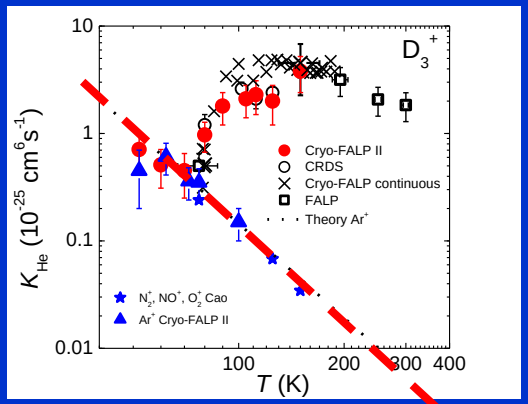

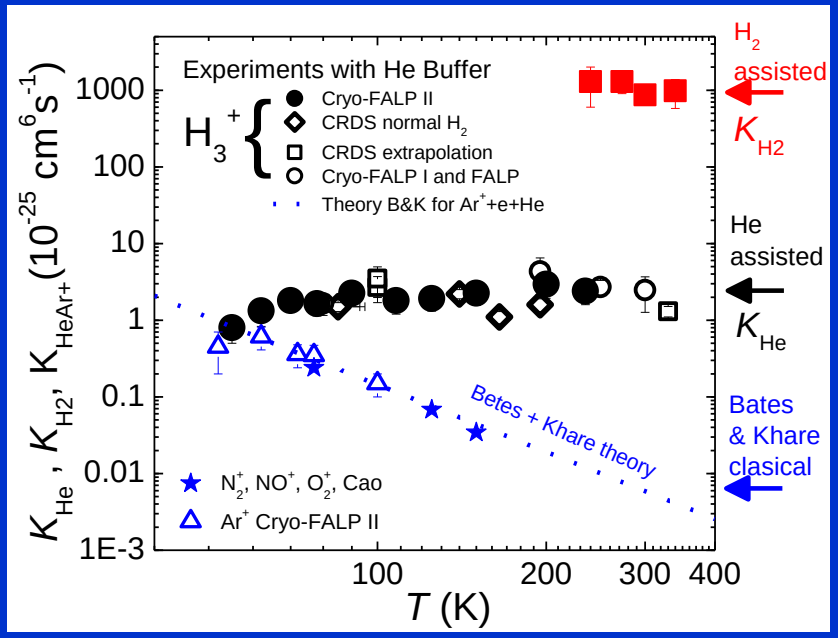

$$H_3^+ + e + He \rightarrow H + H + H + He$$

$$H_3^+ + e + H_2 \rightarrow H + H + H + H_2$$

REALITA všedných dní

$$Ar^+ + e + e \rightarrow Ar + e$$

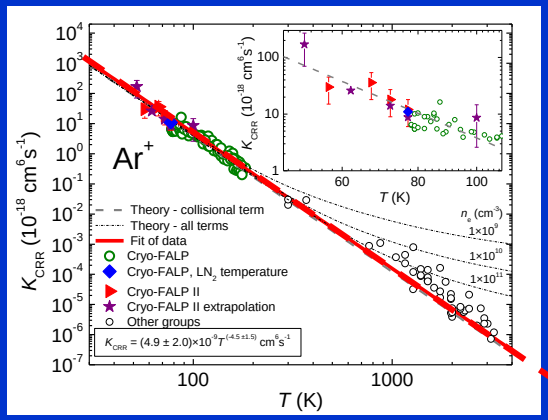

$\sim T^{-4.5}$

$$Ar^+ + e + He \rightarrow Ar + He$$

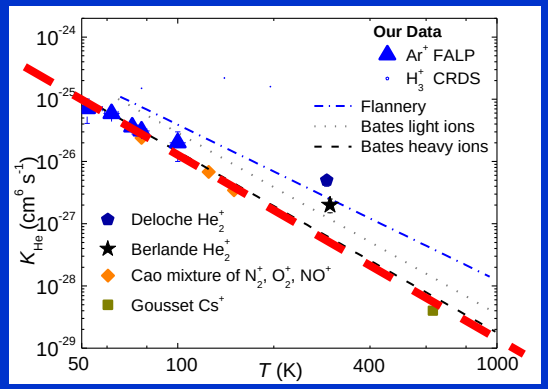

$\sim T^{-2.5}$

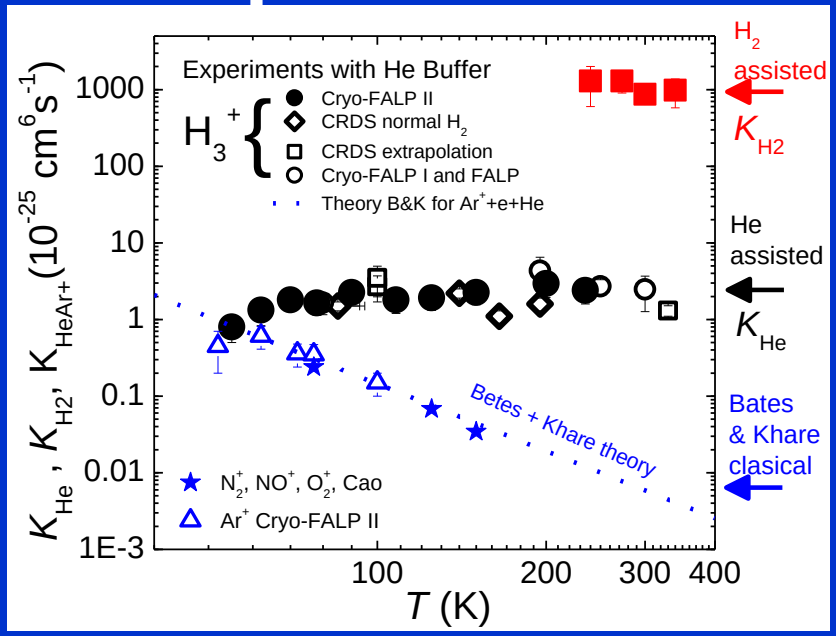

FP II 1- 2018

$$H_3^+ + e + He \rightarrow H + H + H + He$$

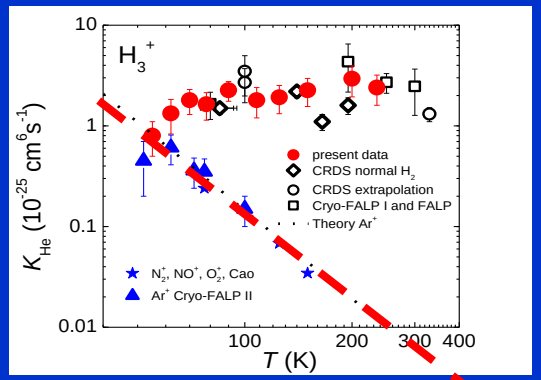

$$D_3^+ + e + He \rightarrow D + D + D + He$$

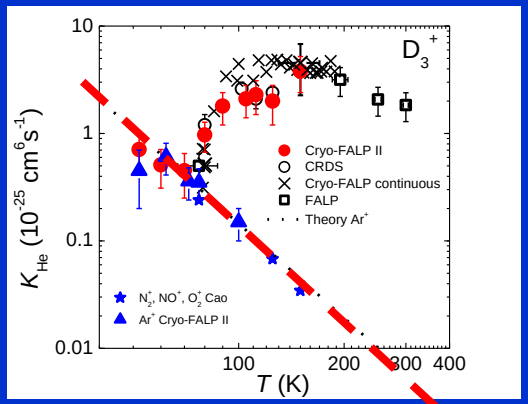

Three-body recombination FP II 1 2018

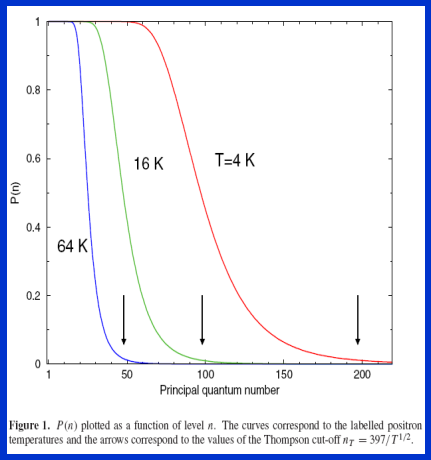

Figure 1. $P(n)$ plotted as a function of level n. The curves correspond to the labelled positron temperatures and the arrows correspond to the values of the Thompson cut-off $n_T = 397/T^{1/2}$.

$$A^+ + e + e \rightarrow A + e$$

B Zygelman , Department of Physics, University of Nevada Las Vegas, Las Vegas, NV 89154, USA

Abstract: The formation of antihydrogen atoms via three-body recombination (TBR) of antiprotons with positrons is considered. A collisional radiative model for the recombination process is employed to study the time dependence of stateresolved antihydrogen populations. We show that at low temperatures $T^{-9/2}$ scaling of theTBRcoefficient does not characterize the total recombination rate, and an alternative expression for the three-body rate coefficient is proposed. (Some figures in this article are in colour only in the electronic version)

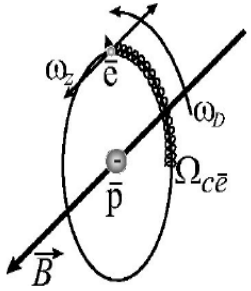

FIG. 1. Drawing of a guiding center drift atom. In order of descending frequency, the positron executes cyclotron motion, oscillates back and forth along a field line in the Coulomb well of the antiproton, and $\mathbf{E}\times\mathbf{B}$ drifts around the antiproton.

S. G. Kuzmin and T. M. O'Neil

Department of Physics, University of California at San Diego,

Motion of guiding center drift atoms in the electric and magnetic field of a Penning trap

This paper discusses the motion of the weakly bound atoms in the electric and magnetic field of the plasma and trap. The effective electric field in the moving frame of the atom polarizes the atom, and then gradients in the field exert a force on the atom. An approximate equation of motion for the atom center of mass is obtained by averaging over the rapid internal dynamics of the atom.

Quo vadis ?

$$H_3^+ + e^- \xrightarrow{\alpha_{Bin}} H_2 + H, .H + H + H$$

$$H_3^+ + e^- \underset{\tau_a}{\overset{\alpha_F}{\rightleftarrows}} H_3^{\#} \xrightarrow{H_2 \ldots . ks_{H2}} \text{neutrals}$$

$$H_3^{\#} \xrightarrow{He \ldots . ks_{He}} \text{neutrals}$$

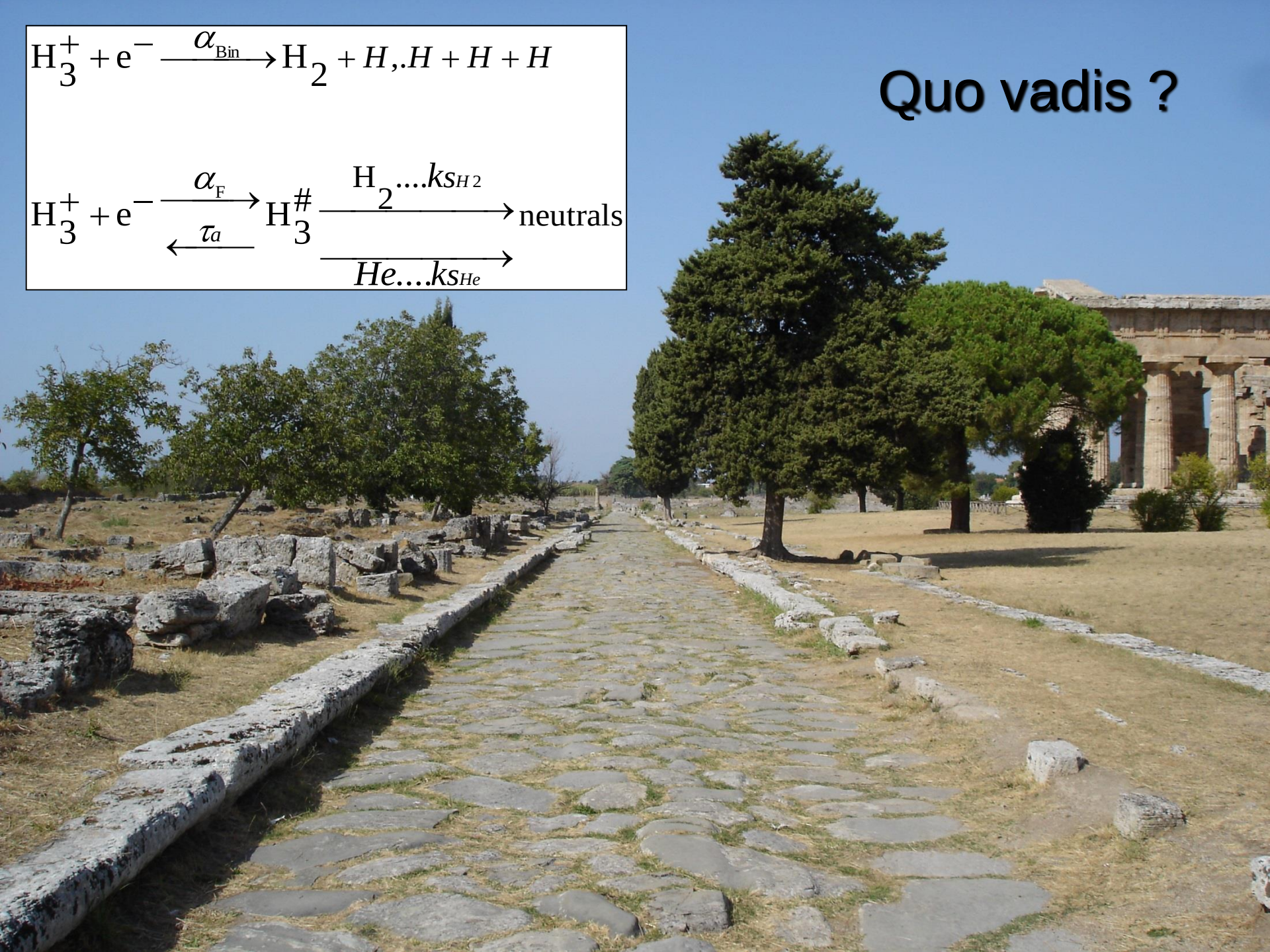

Binary

$$H_3^+ + e^- \xrightarrow{\alpha_{Bin}} H_2 + H,.H + H + H$$

Ternary

$$H_3^+ + e^- \underset{\tau_a}{\overset{\alpha_F}{\rightleftarrows}} H_3^{\#}$$

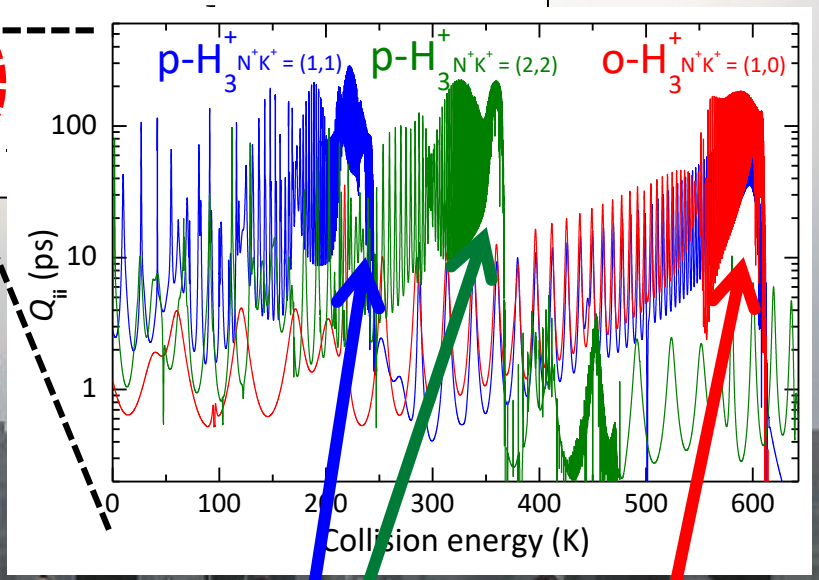

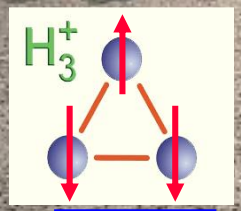

para

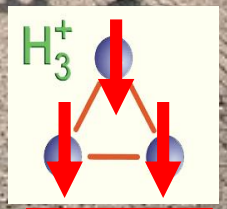

ortho

Laser induced recombination, influence of B and E field

Model

(He/Ar/H_2 mixture)

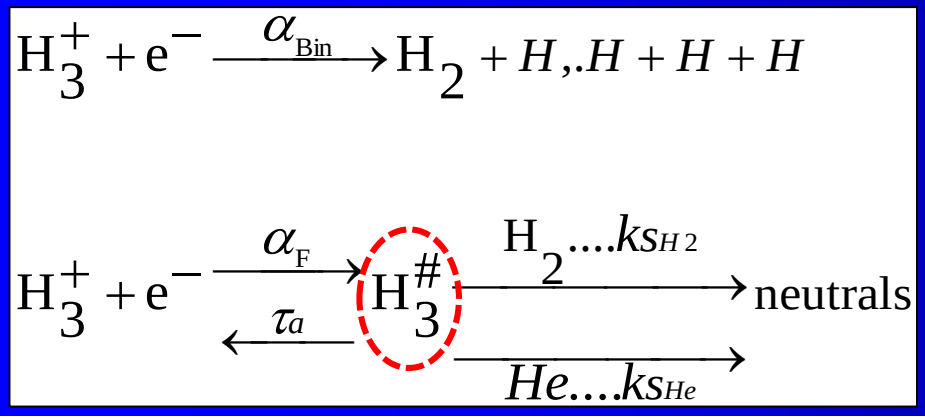

By solving the set of balance equations we obtain:

$$\frac{\partial n_e}{\partial t} = -\alpha_{bin}[H_3^+]n_e - \alpha_F[H_3^+]n_e \frac{k_{SHe}[He] + k_{SH_2}[H_2]}{\frac{1}{\tau_a} + k_{SHe}[He] + k_{SH_2}[H_2]}$$

We introduce:

$$K_{He} = \alpha_F k_{SHe} \tau_a \qquad K_{H2} = \alpha_F k_{SH2} \tau_a$$

$$\alpha_{eff} = \alpha_{bin} + \alpha_F \frac{K_{He}[He] + K_{H2}[H_2]}{\alpha_F + K_{He}[He] + K_{H2}[H_2]}$$

In the <u>low density limit</u> ([He] and [H_2]→ 0), linear approximation

$$\alpha_{eff} = \alpha_{bin} + K_{He}[He] + K_{H2}[H_2]$$

State selective recombination

$$\frac{dn_e}{dt} = -\alpha_{eff} n_e n_+ + \frac{n_e}{\tau_D} = -\alpha_{eff} n_e^2 + \frac{n_e}{\tau_D},$$

$$\alpha_{eff} = \alpha_{eff}(T_e, [He], [H_2])$$

$$\alpha_{eff} = ({}^{p}f_3 . {}^{p}\alpha_{BIN} + {}^{o}f_3 . {}^{o}\alpha_{BIN}) + ({}^{p}f_3 . {}^{p}K_{He} + {}^{o}f_3 . {}^{p}K_{He})[He]$$

SA-CRDS

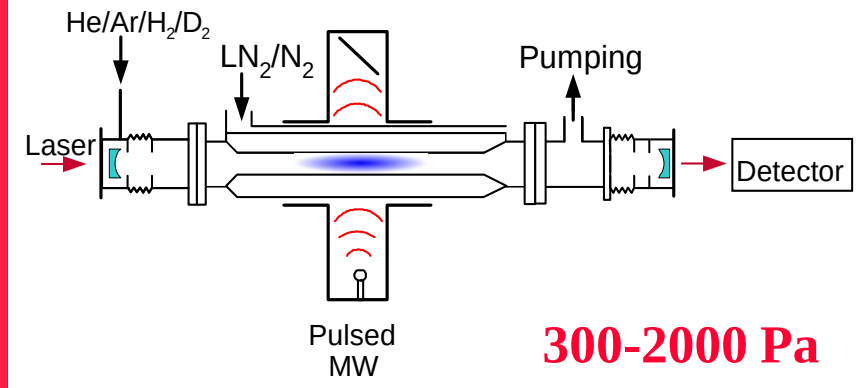

Afterglow in He/Ar/H_2 mixture

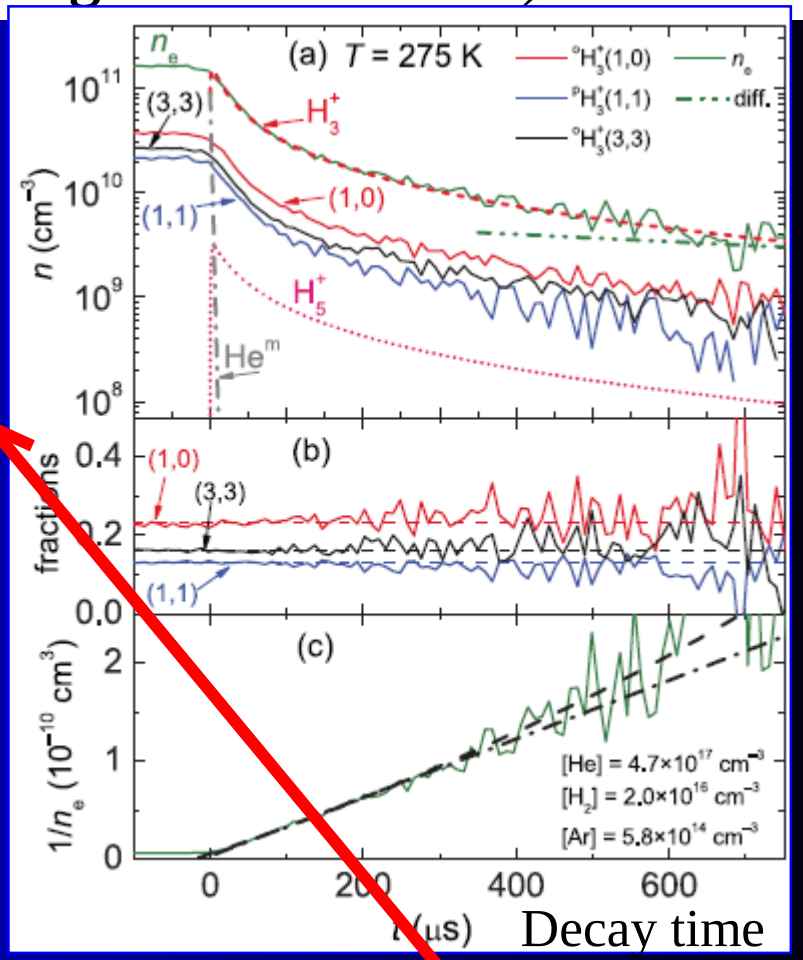

$$\alpha_{eff} = \alpha_{eff}(T_e, T_i, [He], [H_2], {}^{p}f_3, {}^{o}f_3)$$

$\alpha = \alpha(T)$

$\alpha_{eff} = \alpha_{eff}(T_e, T_{kin}, T_{rot}, n_e, [He], [H_2], {}^{o/p}f_2, {}^{o/p}f_3)$

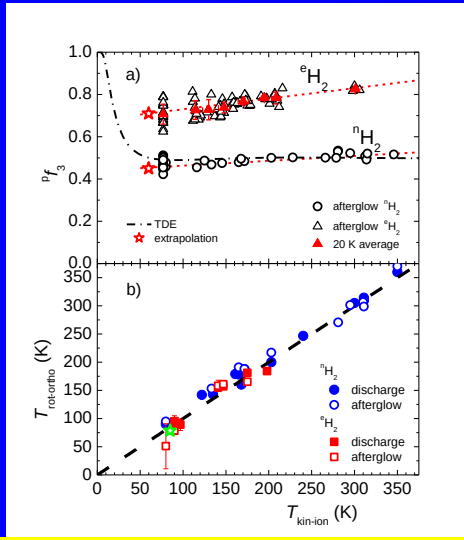

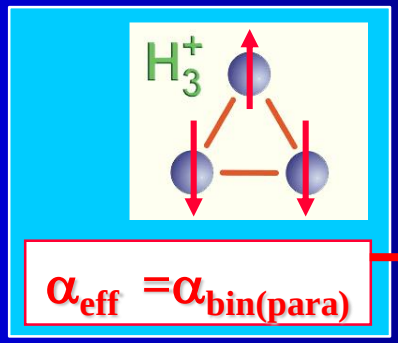

$\alpha_{eff} = \alpha_{bin(para)}$

$\alpha_{eff} = \alpha_{bin\text{-}mix}$

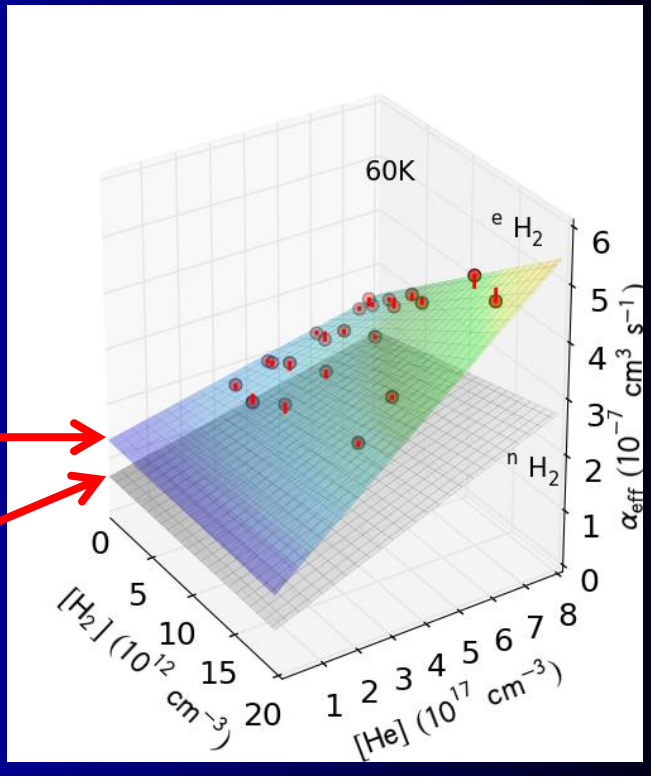

$T = T_{wall} = T_{He} = T_e = T_{rot} = T_{kin\text{-}ion}$

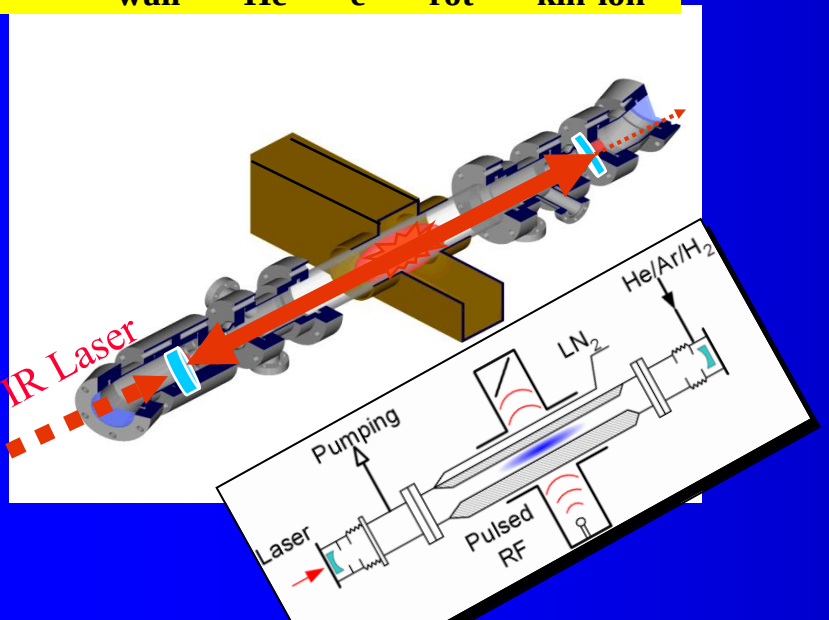

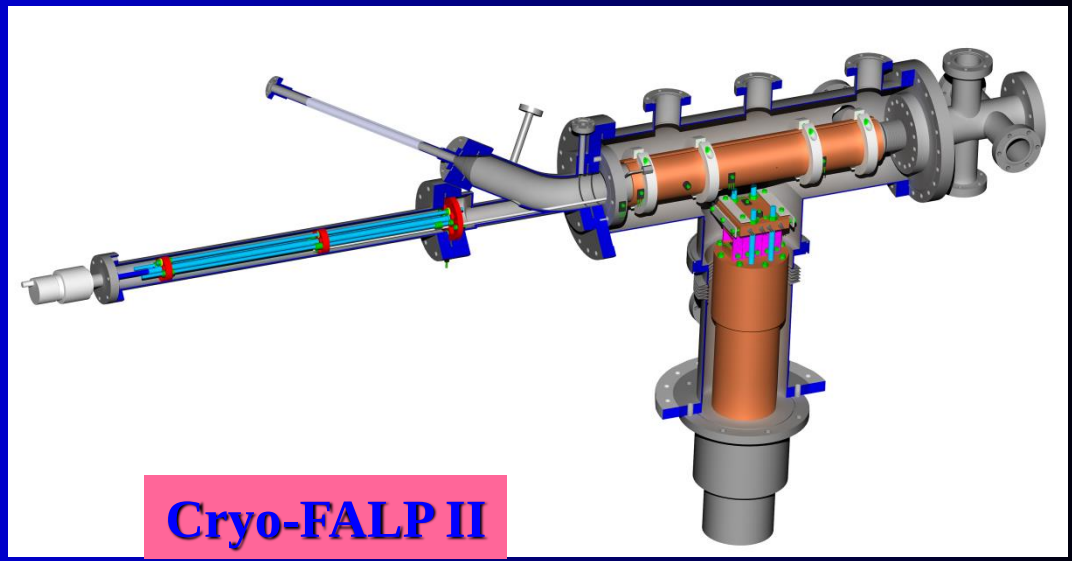

model

$$H_3^+ + e^- \xrightarrow{\alpha_{Bin}} H_2 + H, .H + H + H$$

$$H_3^+ + e^- \underset{\tau_a}{\overset{\alpha_F}{\rightleftarrows}} H_3^{\#} \xrightarrow{H_2 \ldots . ks_{H2}} \text{neutrals}$$

$$\xrightarrow{He \ldots . ks_{He}}$$

para-H_3^+ and orto-H_3^+

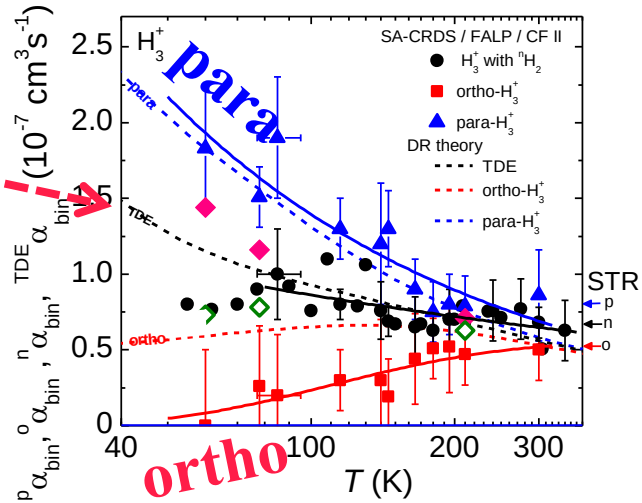

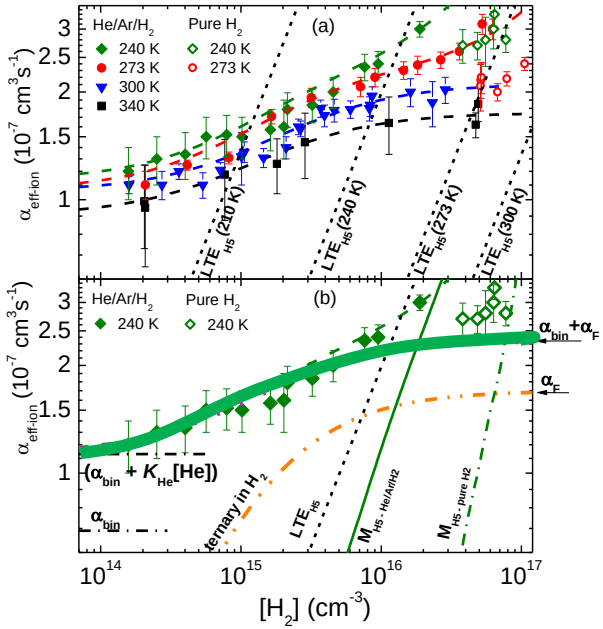

SATURATION

$$\alpha_{eff} = \alpha_{bin} + \alpha_F$$

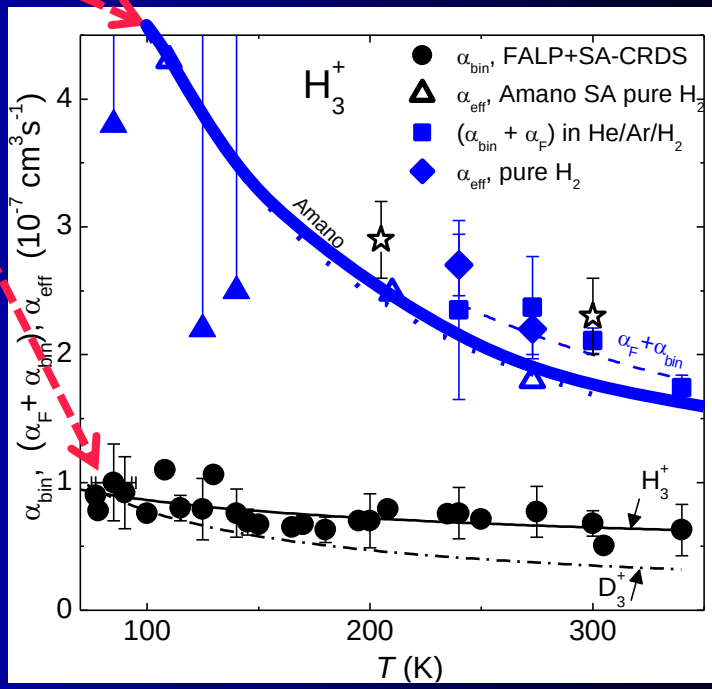

$$\alpha_{eff} = \alpha_{bin} + \alpha_F \frac{K_{He}[He] + K_{H2}[H_2]}{\alpha_F + K_{He}[He] + K_{H2}[H_2]}$$